VALIDATION OF THE BOUNDARY LAYER REPRESENTATION IN THE ECMWF MODEL

Anton C M Beljaars[1] and Alan K Betts[2]

[1]European Centre for Medium-Range Weather Forecasts
Shinfield Park, Reading, UK

[2]Atmospheric Research, Pittsford, VT 05763, USA

1. INTRODUCTION

In this paper we concentrate on the boundary layer budgets of heat and moisture over land. The boundary layer (BL) is the region between the surface and the free atmosphere where vertical diffusion due to turbulent motion takes place. The BL parametrization determines together with the land surface scheme the surface fluxes of heat moisture and momentum and redistributes these fluxes over the boundary layer depth. A realistic representation of the boundary layer in large scale models is important because (i) the large scale atmospheric budgets are affected on a time scale of a few days through the surface fluxes, (ii) the boundary layer interacts with other processes e.g. clouds, radiation, convection and (iii) boundary layer variables are important forecast products. The latter is obvious for wind at the 10 m level and the temperature at screen level, but also more and more use is made of advanced boundary layer parameters such as surface fluxes, boundary layer height and boundary layer wind fields. These parameters are for instance needed to compute diffusion and advection of air pollution. In this paper we will try to assess the quality of BL related parameters in the ECMWF model like surface fluxes of heat and moisture, boundary layer depth and thermodynamic structure. The main comparison is with FIFE data (Kansas, USA, see *Sellers et al.*, 1988) for August and October 1987, but we will also show some results from a comparison with data from Cabauw in the Netherlands and operational radio sondes over Europe. On the basis of these comparisons a number of model deficiencies were identified, which have led to the development of a revised boundary layer scheme. It will be shown how the new parametrization improves the results and which problems remain to be solved.

2. COMPARISON WITH FIFE DATA

During 1987 an extensive series of surface data was collected (*Sellers et al.*, 1988) over the Konza prairie in Kansas during the First ISLSCP (International Satellite Land Surface Climatology Project) Field Experiment (FIFE). This data was gathered over an area of 15 x 15 km, reduced to a single mean time series (*Betts and Ball*, 1992) and compared with time series of the closest grid-point from ECMWF model forecasts. Short range forecasts (48 hours) were selected for this comparison based on the idea that large scale meteorological features are fairly accurate in this time-range and that at the same time the boundary layer has had enough time to adjust to its forcing (boundary layer processes are relatively fast). To resolve the diurnal cycle it was necessary to rerun the model with diagnostics that archive model variables and fluxes every time step for selected grid points. A recent model version was used (cy38 with physics updates for cy39) which was started from the operational analysis of October 1987. For August 1987 the

re-analysis, performed with the same model cycle, was used. Unfortunately, the re-analysis for August had the wrong deep soil climate field (the June climate, which is much more moist). The surface fluxes of heat and moisture should therefore not be interpreted in the absolute sense, but since they are so close to observations, the boundary layer budget of heat and moisture can still be compared with data to identify other model problems. For more details on FIFE data and the comparison with short range model forecasts we refer to *Betts et al.* (1990,1992,1993), details on the BL parametrization are given by *Louis* (1979) and *Louis et al.* (1982); the land surface scheme is described by *Blondin* (1991).

2.1 October averages

To give some indication of systematic differences in the diurnal cycle between the model forecasts and the data, we averaged 7 days in October, which were predominantly sunny in both data and model. These verifying days ran from 12 GMT on Oct 6 to 12 GMT on Oct 10, and from 12 GMT on Oct 11 to 12 GMT on October 14. Because we have 48-hr forecasts, we can look at the corresponding verifying 7-day average for both the first and second days of the model forecast (referred to as Day 1 and Day 2), to give some indication of the model drift in the first 48 hrs of the forecast.

Fig. 1 compares the diurnal cycle of incoming and reflected solar radiation. The x-axis is 24 hrs starting from 1200 GMT. Local solar noon is about 1820 GMT, or 6.3 HOURS on Fig. 1. Solar radiation in the EC model is higher than in the data, but the differences are even larger on absolutely clear days (in the 7-day average there is some cloudiness in both model and data). The differences between Day 1 and Day 2 of the forecast are small. Fig. 2 shows the albedo: the model has a fixed value at this gridpoint of 0.16, while the two sets of surface data have slightly higher values in the range 0.18 - 0.21 near solar noon. Fig. 3 shows the net radiation (RNet); where the difference between model and data has become larger, partly because of the albedo differences. The data are direct measurements with well calibrated net radiometers. They were well calibrated, since net radiation is critical in the Bowen ratio method for finding the surface fluxes. These independent net radiation measurements support our conclusion that the incoming solar radiation is too high in the model. Note that at night, the net outgoing radiative flux is much higher in the model: this is because the ground surface layer is too warm, and is cooling by longwave radiation.

We show both radiation data averages to give some indication of the uncertainty of the data. However the 'FLUX' radiation averages (shown as solid lines), which show lower incoming solar radiation and a higher albedo, are internally more self consistent: that is the net radiation measured directly most closely balances the sum of the four components measured and averaged separately.

Fig. 4 shows the SH and LH fluxes, with the data as solid lines and the model dotted for Day 1 and dashed for Day 2. The daytime model fluxes are biassed. Even in this average, there is nearly zero LH flux in the

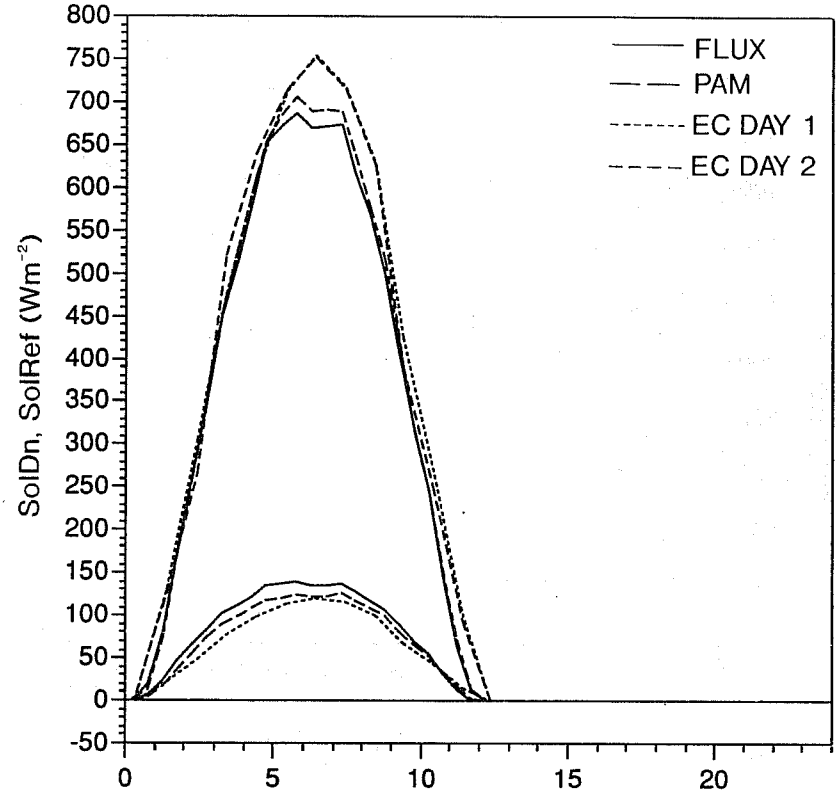

Fig. 1 Incoming and reflected solar radiation for a 24-hr period starting at 1200 GMT for 7-day October 1987 average (FLUX data, solid; PAM data, broken), compared with the average of the EC model forecasts with the same verification dates.

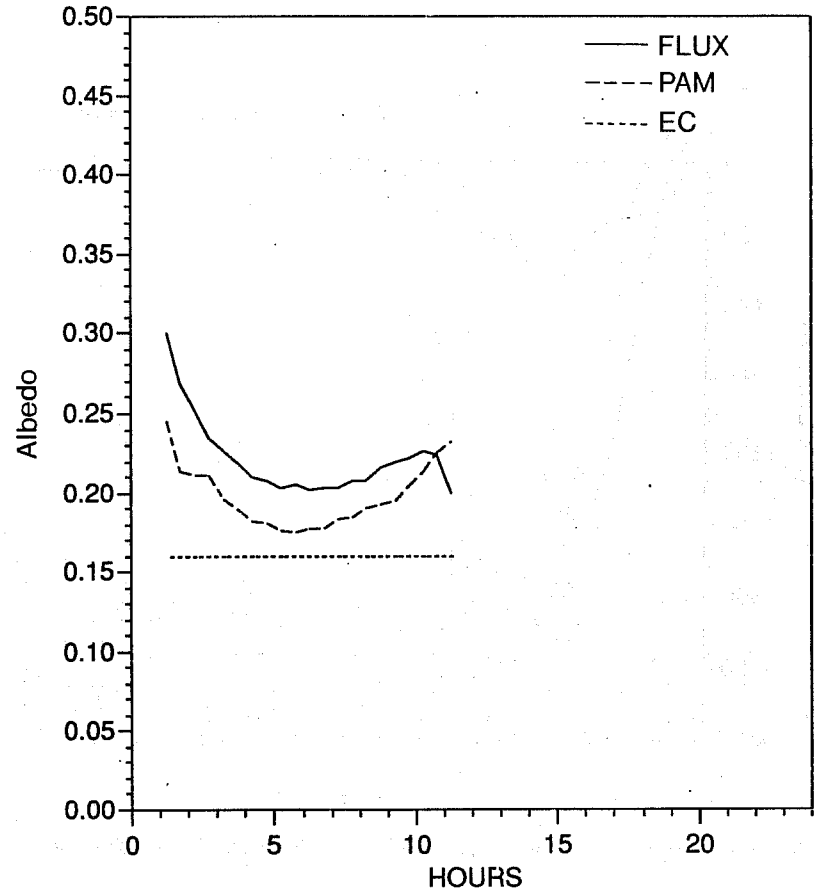

Fig. 2 As Fig. 1 for surface short-wave albedo.

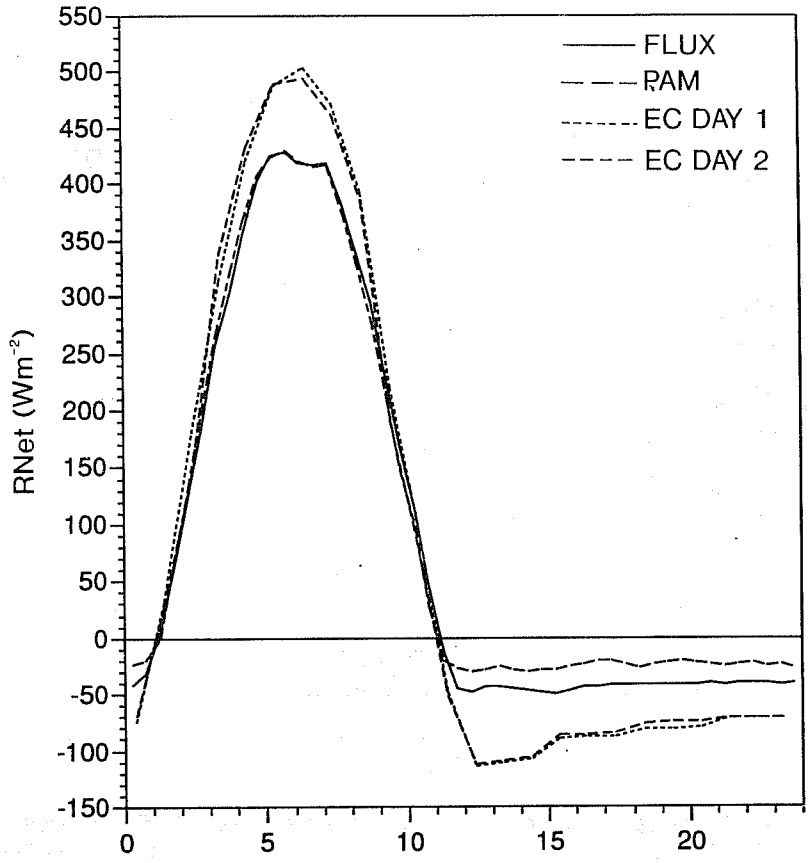

Fig. 3 As Fig. 1 for net radiation.

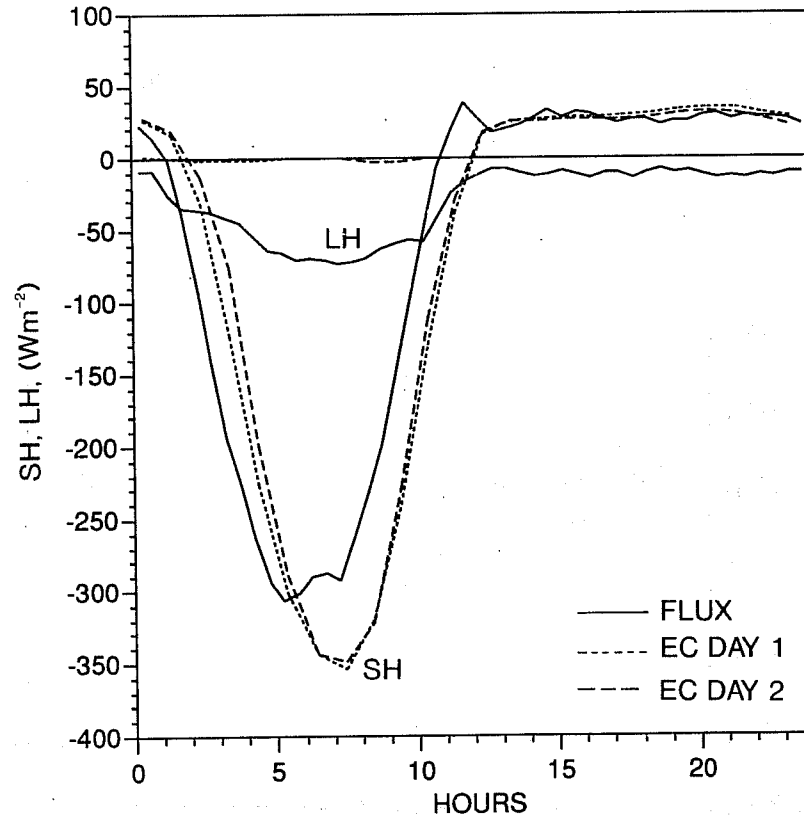

Fig. 4 As Fig. 1 for surface sensible and latent heat flux from FLUX data and EC model.

model, while the SH flux shows a phase shift which results from the too high ground heat flux shown in Fig. 5. Closer investigation showed that part of the ground heat flux error is due to a time truncation problem, although the thermal inertia of the 7 cm thick surface layer is the main reason. The time truncation problem is related to the process splitting between the BL scheme and the land surface scheme. In a single time-step, the BL profiles are integrated forward with an implicit scheme, keeping a constant temperature at the surface. The resulting fluxes are then used for the corresponding time-step with the land-surface scheme. Consequently, when the temperature is rising steeply in the morning, the surface temperature as seen by the BL scheme lags, and is too low. Therefore the sensible and latent heat fluxes are also too low, and the residual of the surface energy budget shows up as a time-truncation error in the ground heat flux, giving the sharp morning peaks in Fig. 5 (see *Beljaars*, 1991 for a discussion of the numerical schemes of the parametrized physics).

Fig. 6 shows the diurnal response of the 2-m air temperature (TK). The morning minimum in the model is too high, and the difference from the data increases from Day 1 to 2 of the forecast. Fig. 7 compares the 2-m air temperature, and the surface temperature (TSfcK: a radiometric skin temperature for the data, and that of the 7 cm ground layer for the model) for the data and Day 1 of the model forecast. The temperature difference during the daytime heating cycle between surface and 2 m becomes larger in the data than in the model. This is related to the model surface layer formulation. The model has the same roughness length for heat and momentum, while the analysis of the data (*Betts and Beljaars*, 1992), as well as earlier studies (*Garratt and Hicks*, 1973; *Garratt*, 1978) suggest that the roughness length for heat is at least an order of magnitude less than that for momentum. The large differences in surface temperature at night are partly responsible for the differences in the net radiation (Fig. 3). These different characteristics of the model are significant. The surface temperature and the air temperature at 2 m are closely coupled in the model. During this 24-hr average of 7 sunny days, these model temperatures rise about 2 K, whereas for the observations, the rise is nearer 1 K. The net heat flux into the ground in the model is about 10 Wm^{-2} (averaged over 24 hrs), whereas the observations show (more realistically) an average 24-hr ground flux upward of 3 Wm^{-2}: that is, the ground has started to cool in October. The deep soil temperature in the data is 290 K (at 50 cm); clearly it is conduction from the deep layers which are warming the surface on these sunny days, despite a net ground flux upward. The deep "climate" temperature in the model (below 49 cm) is similar; it is fixed at 289.5 K in October.

Fig. 8 shows the trend of mixing ratio, q, for the data at 2 m, and the model value at the lowest model level 19 (roughly 33 m). (The model does not carry variables at 2 m. The interpolated 2 m temperature is of value, because temperature is available at the surface and at about 33 m (level 19). However, the 2 m model value of mixing ratio is questionable, because it is computed assuming constant relative humidity between surface and level 19, since q is not available at the surface.) The mixing ratio in the data has a

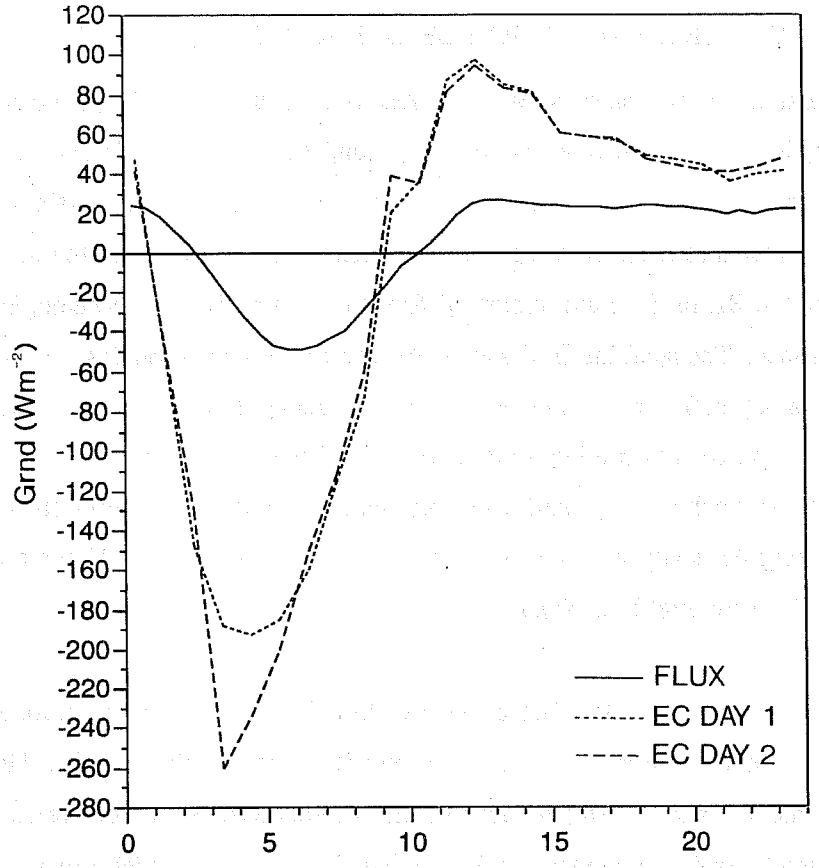

Fig. 5 As Fig. 1 for ground heat flux.

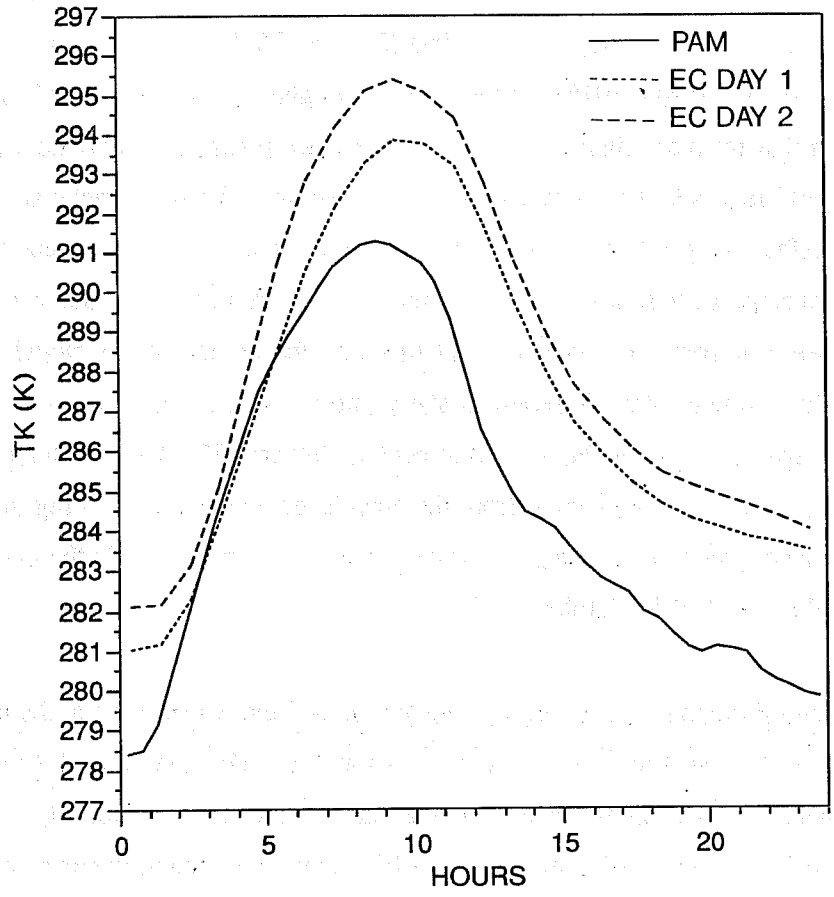

Fig. 6 As Fig. 1 for PAM 2-m air temperature and EC forecast.

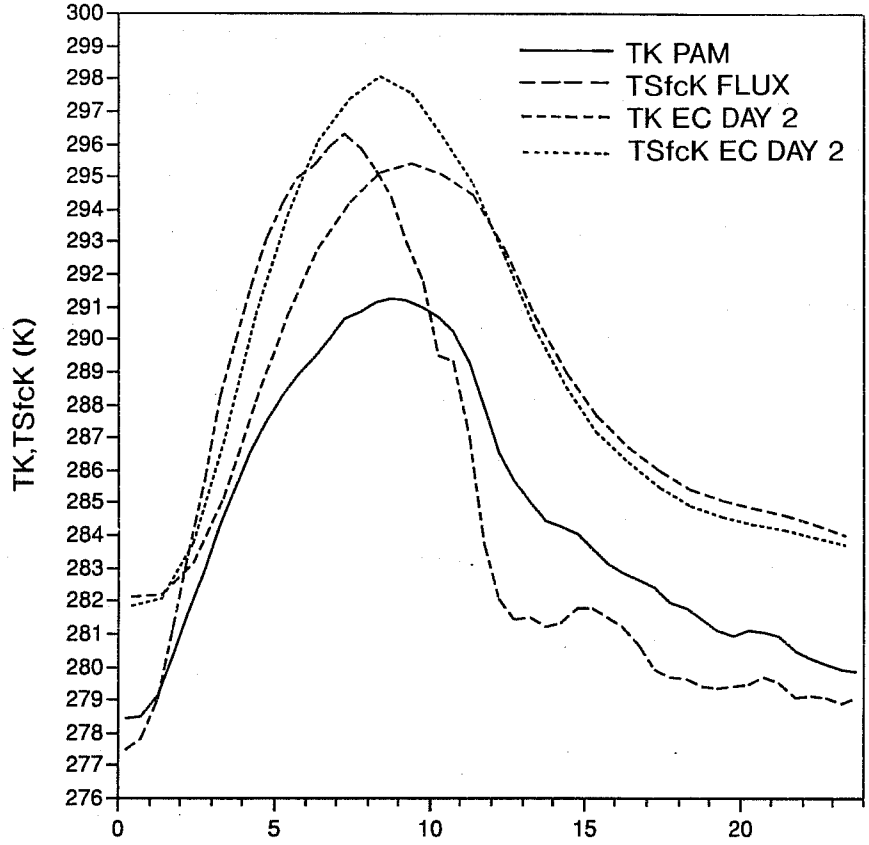

Fig. 7 As Fig. 1 for surface temperature and 2-m air temperature.

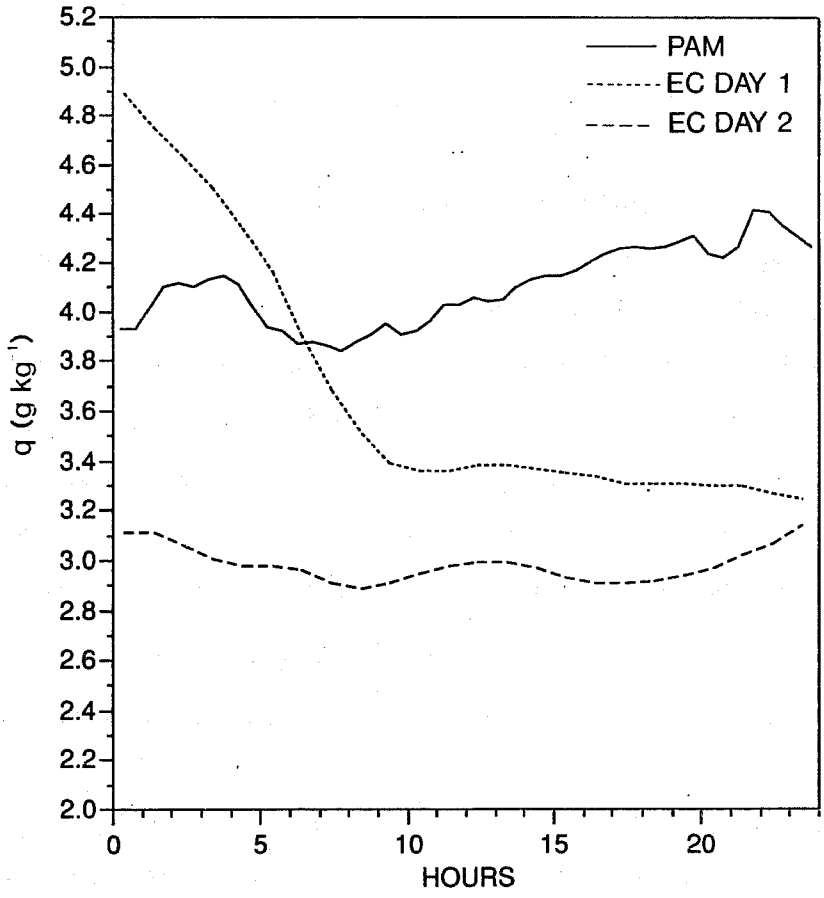

Fig. 8 As Fig. 1 for mixing ratio.

small trend, but the model dries rapidly in the first 24 hrs and then stays dry. This is presumably because there is no surface evaporation.

This October average shows a consistent picture reflecting 5 systematic errors in the model.

(a) The incoming solar radiation is too high in clear sky conditions, perhaps by as much as 10%. The fixed model albedo is lower than the data in October (this difference is less in August: see later), but this may be unique to this gridpoint.

(b) The ground surface model, which has a 7 cm thick first surface layer, is too slow to respond to the net radiation after sunrise, and cools too slowly at night. Since this layer must warm before the sensible heat transfer to the atmosphere can become upward, the model needs a very large downward ground heat flux after sunrise, as large as 200-250 Wm^{-2}. (The error is amplified by a time-truncation problem in the model.) This introduces a daytime phase lag into the upward SH flux, and appears also to result in a net heat flux into the ground, even as late in the year as October.

(c) The difference between surface temperature and air temperature is too small in the model. This is associated with having the same roughness lengths for heat and momentum in the model.

(d) The model LH flux is near zero in October. This results from ground moisture values below the model threshold for evaporation (set at 30% of the soil field capacity). These are kept low by the soil moisture specified in the climate layer for October.

(e) The model BL dries out as a result of having no surface LH flux.

This drift of the model BL towards higher temperature and lower q is summarized on a $(\theta-q)$ plot in Fig. 9. This shows the day-time hourly averaged values of (θ,q) for the data (solid), and for the model (dotted for Day 1; dashed for Day 2). The model data is at level 19 (roughly 33 m), while the FIFE surface data is at 2 m. The numbers denote time in GMT; 12 denotes an average for the hour 1200-1300 GMT. Local solar noon is about 1820 GMT. We see the FIFE data trace a path of almost constant q from morning θ minimum to afternoon θ maximum near 2100 GMT, when the surface starts cooling. The EC model data, however, move towards a warmer and drier diurnal cycle with time; and reach a maximum temperature later, near 2300 GMT. The long dashed lines are isopleths of θ_E. These show that the BL reaches an afternoon maximum in θ_E of 307 K in both model and data. We shall find contrasting results in some August averages.

In October, conditions are very dry: the surface LH flux is small, and BL mixing ratios are around 4 g kg^{-1}. In the next section, we shall show some August comparisons, when the observed evapo-transpiration is

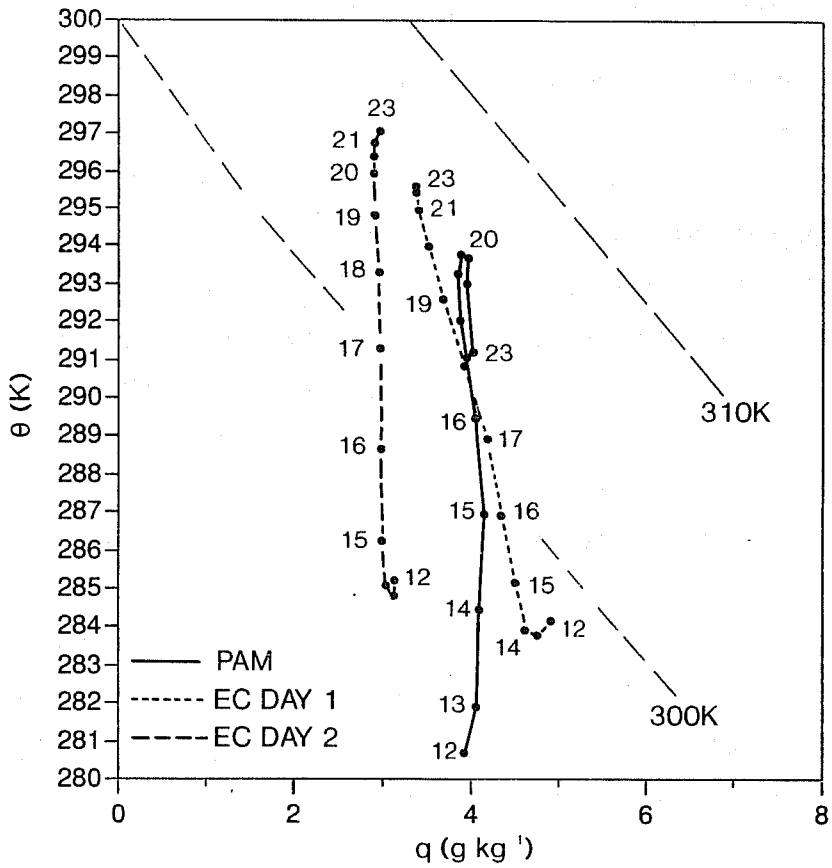

Fig. 9 Daytime (θ-q) plots for data at 2-m , and EC model level 19 (33m) for 7-day October average. Isopleths of θ_E are shown as long dashes. Numbers are hours in GMT; 12 denotes an average for the hour 1200-1300 GMT.

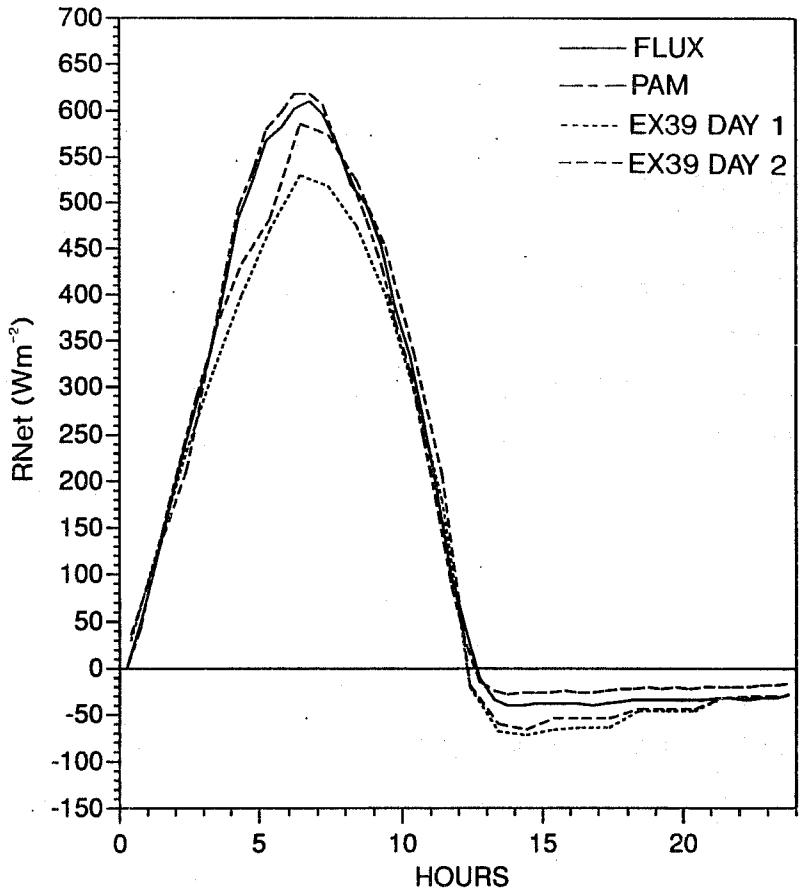

Fig. 10 Net radiation comparison for the 9 day August average started from the experimental re-analysis.

large. This shows up other errors in the model related to the evaporation and soil moisture balance, and to BL-top entrainment.

2.1 August averages from the experimental analysis

This comparison covers the period from August 6-21, 1987. We shall show a 9-day forecast composite started from an experimental re-analysis (also with Cy39 of the model) for a set of mostly sunny days with little rain. This comparison is not as easy as in October, because of significant differences in cloud and rainfall between the observations and the forecasts. There are 9 days with little cloud and no significant daytime rainfall in data and the model: August 6,7,9,10,15,16,17,19,21. Many of these had significantly more cloud in the model forecasts than observed.

Unfortunately, the experimental re-analysis from which the forecasts were started, had by mistake the wrong deep temperature and deep soil climate. The climate for the month of June was used for the July and August assimilation. Although this climate was colder and more moist than the "correct" climate (from *Mintz and Serafini*, 1989), its soil moisture turned out to be quite close to observations at the FIFE gridpoint. As such it helped to produce realistic sensible and latent heat fluxes from the surface (see *Betts et al.*, 1993 for a comparison between forecasts from the operational analysis and the experimental re-analysis). Because of the realistic forcing from the surface, these model runs from the experimental re-analysis are useful in identifying other model problems.

Fig. 10 shows the net radiation comparison between the data and the model composite. In contrast to Fig. 3 (for the October comparison), the model has now less incoming net radiation than the data. This is due to an increase in cloudiness in the model, associated with a moister BL (see below). Fig. 11 shows the sensible and latent heat flux comparison between the flux data and the forecast composite. We see again a phase error in the diurnal cycle but the midday maximum is fairly close to the data. The temperature at 2 m (TK) and the mixing ratio in the boundary layer, however, are not well simulated. The maximum temperature is too low (Fig. 12) and the boundary layer is too moist (Fig. 13). Fig. 14 presents a summary on a (θ-q) plot. In comparison with the data, the model moves towards a moister afternoon state, with an afternoon maximum of θ_E that is 4-5 K higher than the data. Since the surface SH and LH fluxes agree quite well, this suggests another error in the model. The surface fluxes increase θ_E in the BL. If the afternoon equilibrium has too high a θ_E, this means that the downward mixing of low θ_E air in the model must be too low. In fact the EC model has very little BL entrainment, and, as we shall see in the next paragraph, the biases in θ_E and q in Fig. 14 are related to BL depth.

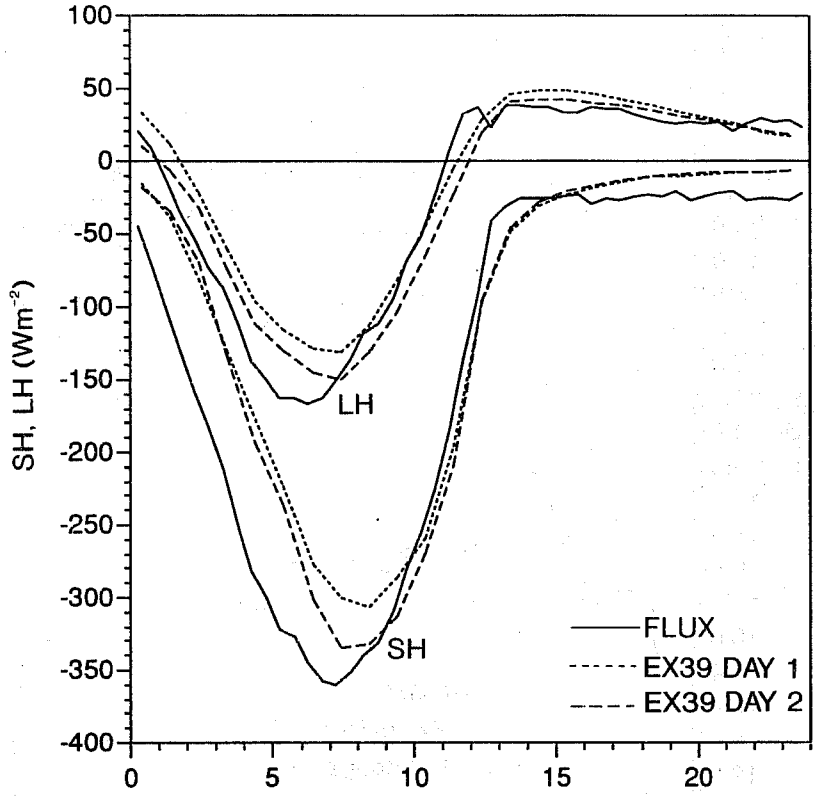

Fig. 11 As Fig. 10 for sensible and latent heat flux.

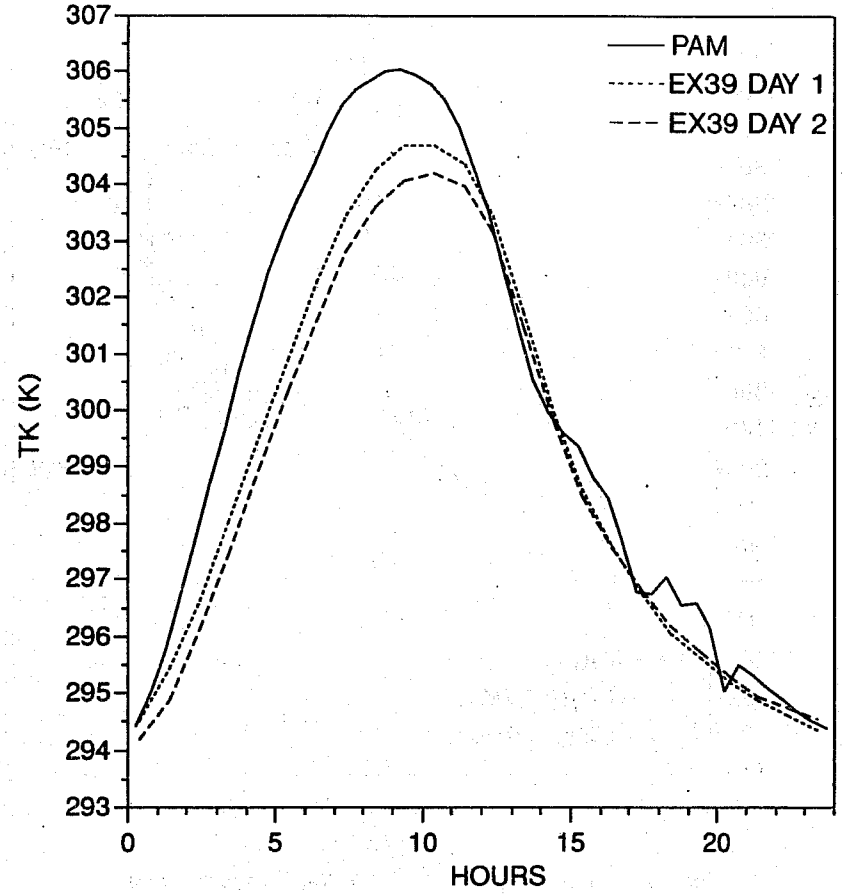

Fig. 12 As Fig. 10 for temperature.

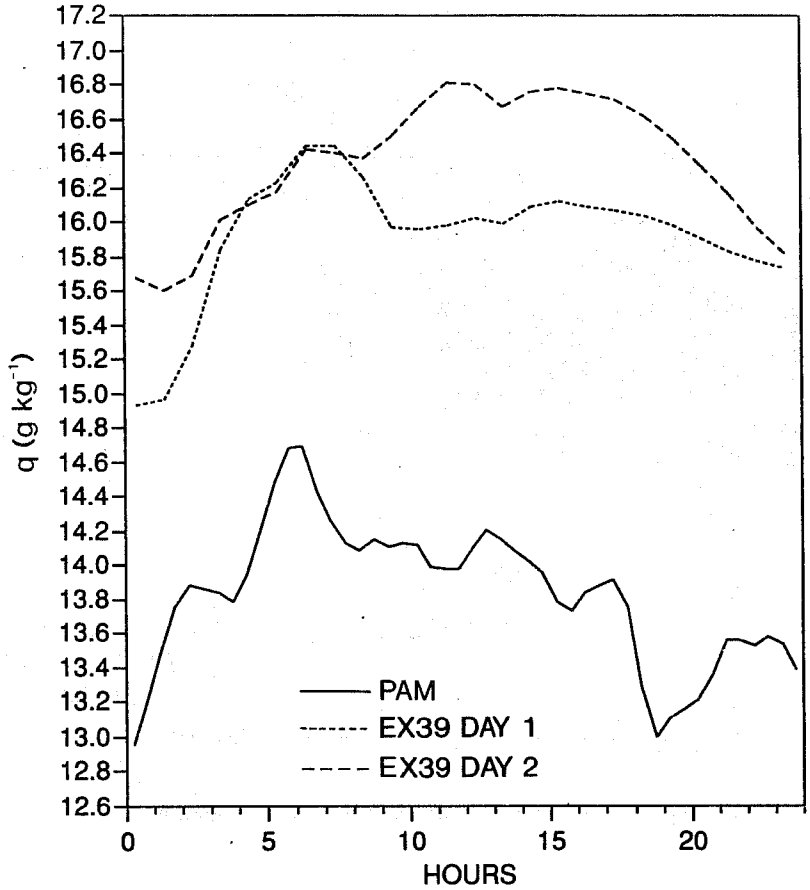

Fig. 13 As Fig. 10 for mixing ratio.

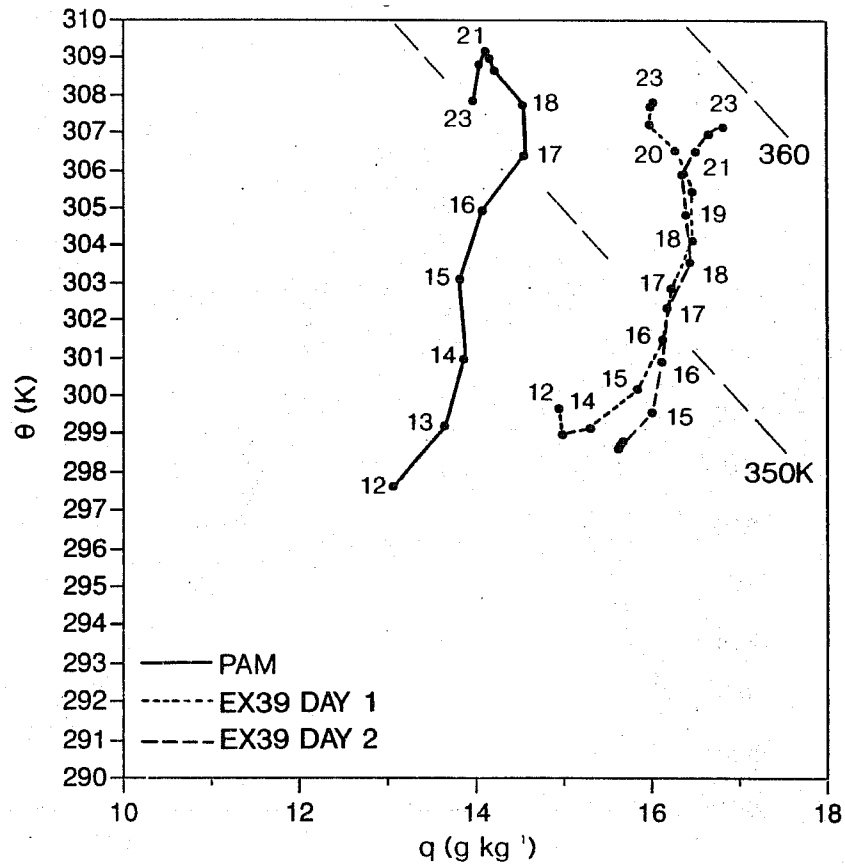

Fig. 14 Daytime (θ,q) plot for the 9 day August average.

The August averages of model forecasts and observations differ significantly in BL structure and evolution. Near the surface (level 19 at 33 m), Figs. 12, 13 show that the model is too cold and moves towards a more moist state (from a too moist initial condition), than the data. The BL profiles reflect these drifts. Fig. 15 shows the θ and q profiles (dotted or dashed) compared with averaged sonde data (solid).

The model profiles are hourly averages, for the hour starting at the GMT time shown. For the observations we used the radiosondes which were launched at roughly 90-min intervals on these 9 days (the mean launch times are shown). The BL profiles (for both data and the model) were scaled in pressure using BL depth, and interpolated to scaled pressure levels before averaging. This preserves the vertical structure within the BL in the composite (*Betts*, 1976). For the model, which has a relatively coarse vertical resolution of order 25 mb, this definition of BL-top is much less exact: we chose the middle of the first stable layer. As a result of this coarse vertical resolution, the model averages have much smoother profiles.

Fig. 16 shows BL-top as a function of time for the data (solid) and the model (Day 1 dotted, Day 2 dashed). The model BL top grows at barely 60% of the rate observed. Since the surface fluxes of sensible and latent heat are reasonably close to observations, it is believed that the errors in BL structure are related to the lack of entrainment. Cycle 39 of the EC model has very little diffusion through stable layers, since diffusion coefficients are calculated using a local Richardson number closure (*Louis*, 1979). Hence there is effectively no entrainment at BL-top. The BL does grow by encroachment as the surface warms. Without entrainment, the model BL grows much too slowly, and drifts to a moist and cold state, since less warm dry air is incorporated into the BL.

In the data, BL mixing ratio is a very stable balance between surface evaporation and BL-top entrainment of dry air (Fig. 14). To get these right in the model is not easy: it requires an entrainment parametrization, and the right surface energy balance, which itself depends critically on the soil moisture. In turn, biases in the model q and θ_E, produce biases in the diurnal cycle of cloud and rainfall.

2.3 Comparison of mid-day evaporative fraction

Over the grassland hills of FIFE, the surface evaporation is controlled largely by evapotranspiration, except immediately after rain, when the surface is wet. On successive days without significant rainfall, soil moisture falls. Natural grassland appears to maintain a high level of evapotranspiration for long timescales: of order 7-10 days or longer (see *Kim and Verma* 1990 for FIFE, and *Gash et al.* 1991 for fallow Sahelian savannah). It appears that the model parametrization of evaporation has a shorter timescale of only a few days. This direct comparison is not easy to make, however, because of differences in rainfall and cloudiness between model forecasts and the data. In this section we shall show some selected periods in July. These forecasts were from the experimental analysis for July. The fact that it used the June rather than July deep

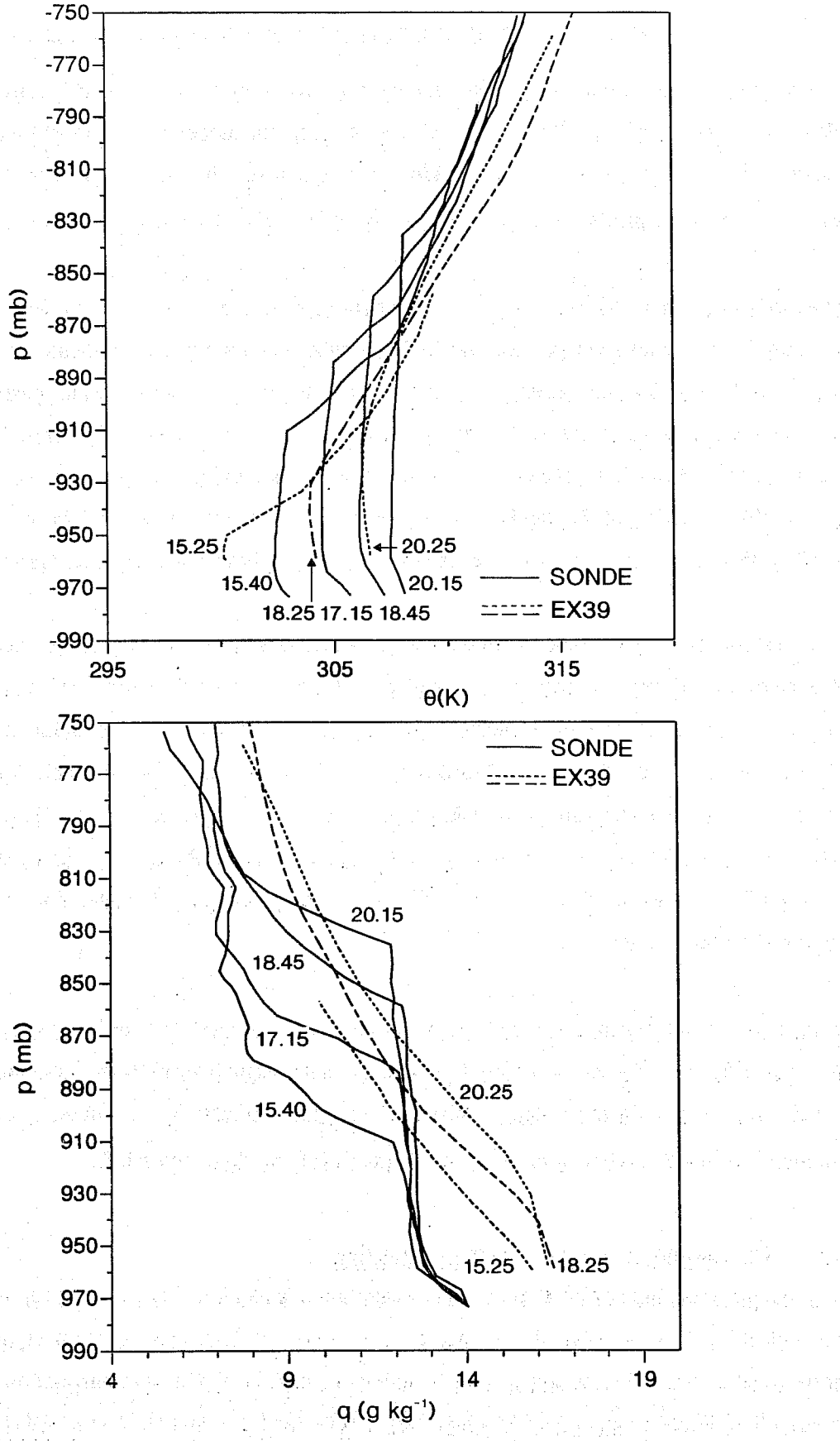

Fig. 15 Comparison of BL profiles of mixing ratio and potential temperature for 9-day August sonde average for GMT times (1540, 1715, 1845, and 2015 GMT) with average EC Day 1 profiles at GMT times shown (1525, 1825, 2025).

climate does not affect our conclusions significantly. The left hand scale of Fig. 17 shows the evaporative fraction, defined as LH/(SH+LH), averaged for the period 1600-2000 GMT (centred near local solar noon: 1820 GMT) from the surface flux data (solid), and selected periods of the EC forecasts (dotted). July 1-3, 9-11 and 14-16 were days with little or no rain in FIFE. For July 1-4, the EC plots are the first day of the forecast for July 1-3 (it rained on July 2 and 3 in the model, when these were the second forecast day); and the second day forecast for July 4. A significant decrease in evaporative fraction is seen over this 4-day dry period. In contrast, in the data for July 1 and 2, the evaporative fraction is constant, and it rises on July 3, because of cloud cover near local noon.

For the period July 9-16, we show the average evaporative fraction in the model for both forecasts for that date, and we draw attention to 2 periods. For July 10-11, the evaporative fraction fell more in the model than in the data (both periods were without rain in both model and data). It rained on July 12 in the model, and the evaporative fraction fell steadily from July 12-16 as shown. The data shows a little rain on July 12 and 13, and then July 14-16 were dry also. IFC-2 of FIFE ended July 11, but a few flux stations collected data during this inter-phase period. The data from July 12-20 labelled "UK" (see *Stewart and Verma*, 1992) shows that the noon evaporative fraction fell only slightly by July 20. There is no significant rain in this period except for showers on July 12-13 and July 17-18. It is clear from these three periods (and August 5-7, not shown) that the evaporative fraction in the model falls more rapidly than the data on consecutive dry days.

There was no rain in FIFE from July 19 - August 2, 1987. Data from 3 days at one site is shown (*Kim and Verma*, 1990). Unlike the period July 12-20, by July 23-30 the evaporative fraction (at this different site) has fallen substantially as the soil dries. Fig. 17 also shows (right hand scale) the difference ΔT_s (for 1600-2000 GMT) between the radiometric surface temperature and the 2-m air temperature (averaged over the FIFE site from the PAM data). This qualitatively reflects the rise and fall of evaporative fraction with each rain episode. We can follow the rise of ΔT_s through the dry period, until the next rainfall on August 3-4. After July 20, ΔT_s continues to rise for a further 6 days, and then remains steady at about 7 K for about a week. During this period the wind-speed fluctuates in the range 3-7 ms^{-1}. This is the time period when the Verma data shows evaporative fraction ≈ 0.5.

Fig. 17 (using data from *Kim and Verma*, 1990), as well as *Gash et al.* (1991) suggest that the response time before grassland vegetation becomes stressed, and evaporative fraction falls, is more than a week. The time constant for this process in the model (dotted curves in Fig. 17) is only a few days. The reason is the coupling between soil moisture and evaporation in the model. The unstressed canopy resistance to evaporation in this version of the EC model is only 25 s m^{-1}. The FIFE data (*Kim and Verma*, 1990) gave

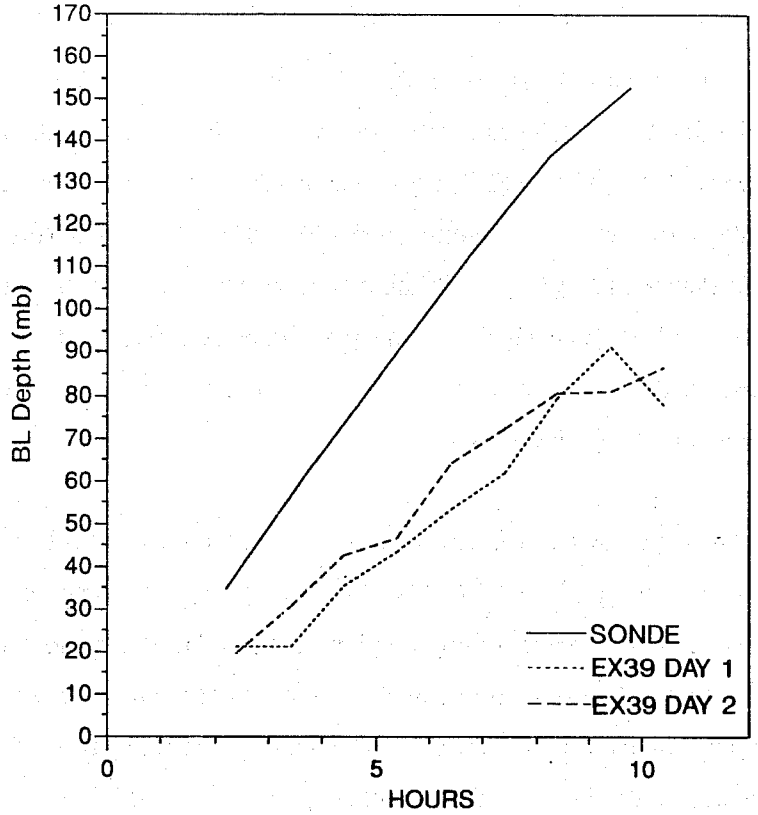

Fig. 16 Comparison of BL-top for 9-day August average; derived from sonde data and Day 1 and Day 2 of the model.

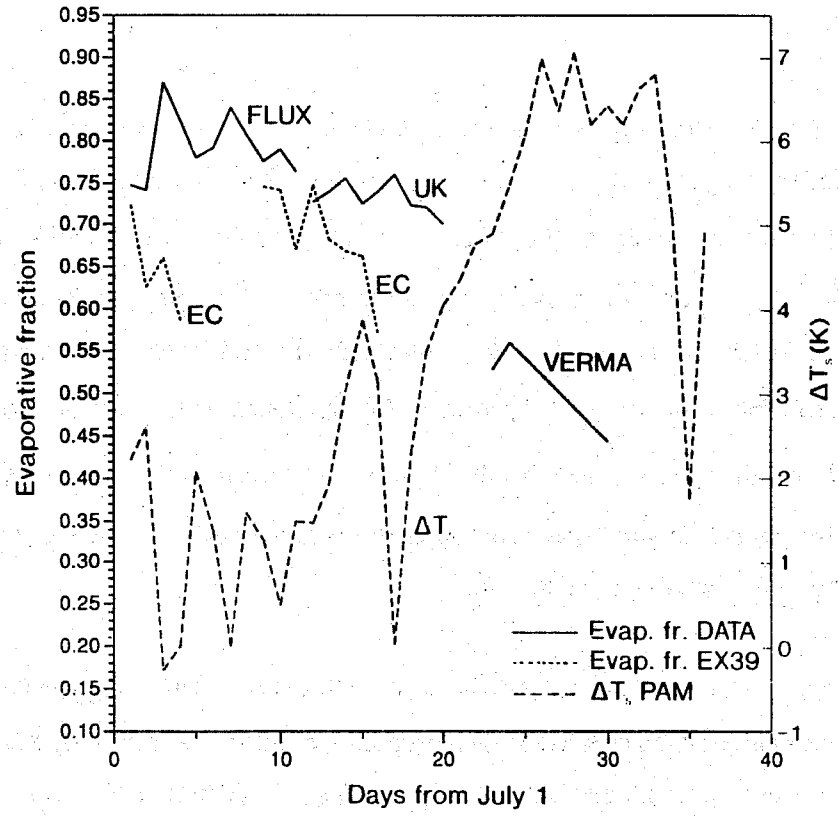

Fig. 17 Comparison of mid-day evaporative fraction from observations and EC model (left scale). Observed difference, ΔT_s, between skin temperature and 2-m temperature for July 1 - August 5 (right scale).

larger values: 75 s m^{-1} in the unstressed conditions on July 11, rising to 300 s m^{-1} in the dry, stressed conditions of late July. In the model the canopy resistance rises and evaporation falls, as the mean soil moisture in the two sub-surface layers (7 and 42-cm deep) falls below 60% of the field capacity. The 7-cm layer dries quickly, giving a short time constant for the fall of evaporative fraction. *Kim and Verma* (1990) and *Gash et al.* (1991) show that the vegetation draws on a much deeper reservoir of soil moisture. In the model the reservoir of water in the 42-cm layer is controlled, not by precipitation, but largely by diffusion of moisture from the model climate layer. This is explored in more detail by *Betts et al.* (1993).

3. REVISED PARAMETRIZATION

The revised parametrization consists of a number of elements that will be documented elsewhere in more detail. Here we limit to the main features:

3.1 Skin temperature

To allow for higher (radiative) surface temperatures during daytime together with lower ground heat fluxes, a skin layer parametrization has been introduced. The skin layer is an shielding layer, representing vegetation, loose material or dry soil, on top of the 7 cm deep soil layer. This layer has no heat capacity and adjusts instantly to the surface heat budget. It is coupled with the underlying soil by means of a conductivity λ_{sk}. The soil heat flux G reads

$$G=\lambda_{sk}(T_{sk}-T_s) ,$$

where T_{sk} is the surface skin temperature and T_s is the temperature of the top soil layer. The second aspect of the skin temperature is its coupling with the atmosphere. We have seen that the radiative surface temperature is too low during daytime with a correct or too high temperature at 2 m. This implies a more loose coupling between surface and atmosphere (higher aerodynamic resistance), which is consistent with the idea of and additional resistance near the surface expressed by a smaller value for the roughness length for heat and moisture than the one for momentum. *Betts and Beljaars* (1992) found a ratio of at least 10 for the FIFE area. In the revised scheme we use a ratio of 10.

3.2 Revised stability functions

A reformulation of the vertical diffusion scheme is desirable for two reasons. First of all the current formulation produces too much diffusion in stable situations. This was the reason to switch the scheme off in the operational model in January 1988 above an estimated upper bound of the PBL height. This is also the reason that the scheme produces stable boundary layers that are too thick by at least a factor two. Secondly, the current scheme does not allow for a consistent treatment of different roughness lengths for momentum, heat and moisture. The need for the latter is becoming more and more evident from

observations over land. Over sea it is necessary to distinguish between momentum and moisture roughness lengths at low wind speeds to reproduce the free convection limit correctly (*Miller et al.*, 1992, *Godfrey and Beljaars*, 1991). The parametrization adopted here is the one proposed by *Beljaars and Holtslag* (1991), where the stability functions are specified as a function of height divided by the Obukhov length. The relation between Obukhov length and Richardson number is solved iteratively in the surface layer; in the outer layer a lookup table is used. The effect of the revised stability functions is to reduce diffusion in stable situations resulting in less surface friction in stable boundary layers and a more shallow stable boundary layer.

3.3 Mixed layer and entrainment formulation

The entrainment parametrization is based on a simple bulk approach, where the buoyancy flux (destruction of turbulence kinetic energy) at the top of the boundary layer is related to the buoyancy flux at the surface. In the inversion we therefore specify the following diffusion coefficients for momentum and heat:

$$K_M=K_H=\{\frac{ds_v}{dz}\}_i^{-1}C_e(w's_v')_s$$

Subscript i stands for the inversion level, subscript s refers to the surface, s_v is the virtual dry static energy $(w's_v')_s$ the virtual dry static energy flux at the surface and C_e the entrainment constant. The numerical value of C_e is 0.4 as suggested by *Betts* (1992) on the basis of FIFE data. To find the inversion level, an air parcel with dry static energy s+ds is lifted dry adiabatically until an inversion is found. The dry static energy s in the mixed layer is incremented with ds to account for the higher temperature in the thermals compared to the surrounding air. The excess energy ds estimated with help of mixed layer scaling:

$$ds=C(w's_v')_s/w_s,\ C=5,$$

$$w_*=\{g/sz_i(w's_v')_s\}^{1/3},$$

$$w_s=\{u_*^3+C_1w_*^3\}^{1/3},$$

where u_* is the friction velocity, w_* the convection velocity scale and z_i the inversion height. The diffusion coefficients in the mixed layer are specified according to similarity profiles proposed by *Troen and*

Mahrt (1986) and slightly modified by *Holtslag et al.* (1990). For $z < z_i$ surface layer scaling is applied:

$$K_M = kzu_*/\phi_M$$

$$K_H = kzu_*/\phi_H$$

where ϕ_M and ϕ_H are the stability functions (see *Beljaars and Holtslag*, 1991) of z/L with L for Obukhov length. For $0.1\ z < z < z_i$:

$$K_M = kw_s z(1-z/z_i)^2,\ k=0.4,$$

$$K_H = K_M/Pr,\ \textit{where}\ Pr = \phi_M/\phi_H\ \textit{at}\ z = 0.1z_i.$$

The reason for specifying a profile of diffusion coefficients in the mixed layer rather than using a local closure as in the *Louis* (1979) scheme, is that in a layer near the inversion the buoyancy flux may be negative due to entrainment and the local closure will switch to the stable parametrization. To avoid this, we simply specify a profile of diffusion coefficients throughout the mixed layer. The exact values of the diffusion coefficients are less important (in either scheme) as long as they are large enough to maintain a well mixed layer.

3.4 Increased vegetation resistance for evaporation

More in line with experimental data, the unstressed vegetation resistance has been increased from 25 to 60 s/m. This is supported by observations during FIFE after rainfall (*Kim and Verma*, 1991) and for grassland and agricultural land (see e.g. *Beljaars*, 1988).

3.5 Comparison of the revised scheme with the operational scheme and data

To illustrate the effect of the new parametrization we show diurnal averages over the nine days in August 1987 that were used in section 2. The new scheme is shown together with the old scheme for day 2 of the forecasts in comparison with data.

The impact of the new scheme on solar radiation is small (Fig. 18); the minor differences are the result of cloud feedback. The net radiation is smaller during daytime and less negative during nighttime (Fig. 19). This is partly due to the increased skin temperature during daytime and a lower skin temperature during the night. The skin layer has the effect of damping the diurnal cycle of the radiative forcing. The sensible and latent heat flux have less phase errors with the new scheme because the skin temperature reacts instantly

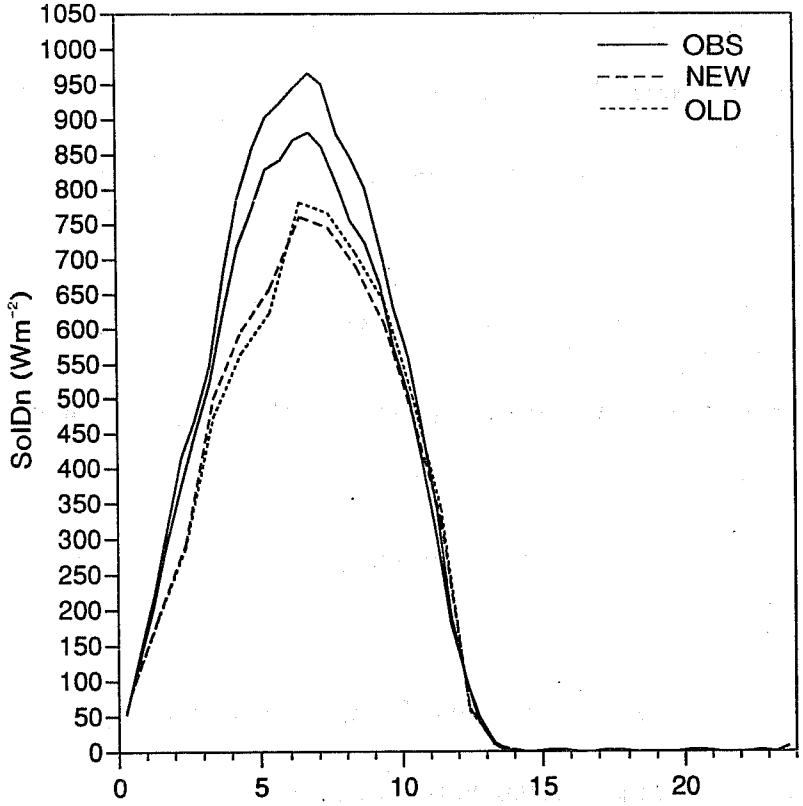

Fig. 18 Incoming solar radiation comparison for the 9 day August average started from the experimental re-analysis for day 2 of the forecasts with the old and the new scheme.

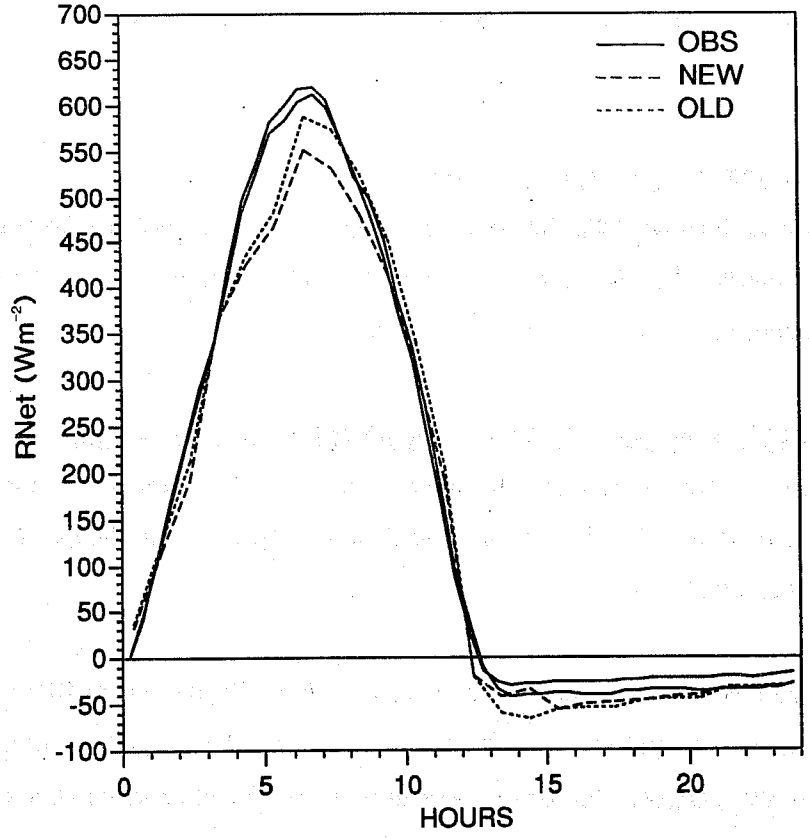

Fig. 19 As Fig. 18 for net radiation.

to the radiative forcing (Fig. 20-21). The ground heat flux has been reduced (Fig. 22) and the diurnal amplitude of the 2 m temperature and the skin temperature have increased and are now in better agreement with the observations (Fig. 23-24). A considerable improvement is seen in the moisture content of the boundary layer. The boundary layer has become much dryer with the new scheme which is mainly due the entrainment of dry air from above the boundary layer (Fig. 25). The boundary layer depth has also improved, but is still too low particularly in the morning hours and at day 2 (Fig. 26).

3.6 Comparison with Cabauw data

Some of the forecasts for the FIFE experiment were also used to compare with data from Cabauw in The Netherlands. Cabauw is located at 51°58'N and 4°56'E in a flat area with grass as the dominant surface cover (*Driedonks et al.*, 1978) and has a 200 m high instrumented meteorological mast. Apart from surface observations of different components of the energy budget, profiles of wind, temperature and moisture are measured. Surface fluxes are inferred from the profile and Bowen method.

The comparison with Cabauw data has two interesting aspects. First of all, the hydrological situation is quite different from FIFE, because the vegetation is only rarely stressed by lack of soil moisture and secondly, the observations up to 200 m allow verification of the lowest 2 model levels (level 18 at about 150 m and level 19 at about 30 m).

It was extremely difficult to find days with little cloud contamination in model and data. Three days have been selected during which cloud cover was not a dominant feature. Some differences between model and data are still related to differences in cloudiness as can be seen from the solar downward radiation (Fig. 27a). The model (with old as well as the new BL scheme) overestimates cloudiness in the morning leading to an underestimation of the solar radiation. For the afternoon we see the opposite effect i.e. the model has less clouds than observed. This leads to an apparent phase shift in the diurnal cycle. The overestimation of the maximum solar radiation leads obviously to an overestimation of the net radiation, but the difference is in fact larger than expected. There are two reasons: (1) the albedo is 0.18 in the model whereas observations indicate 0.23 for this location, (2) the thermal radiative cooling is too low during daytime because the surface temperature is too low and the forecasted cloud cover is too high. The radiative cooling from the surface has been improved with the introduction of the skin temperature. Also the nighttime radiative cooling has been improved considerably with the new scheme; the skin layer allows the radiative surface temperature to drop deeper, resulting in less cooling.

The sensible and latent heat fluxes are too large with both schemes, mainly due to an overestimation of the net radiation (Fig. 28a,b). The latent heat flux is better with the new scheme but the sensible heat flux is

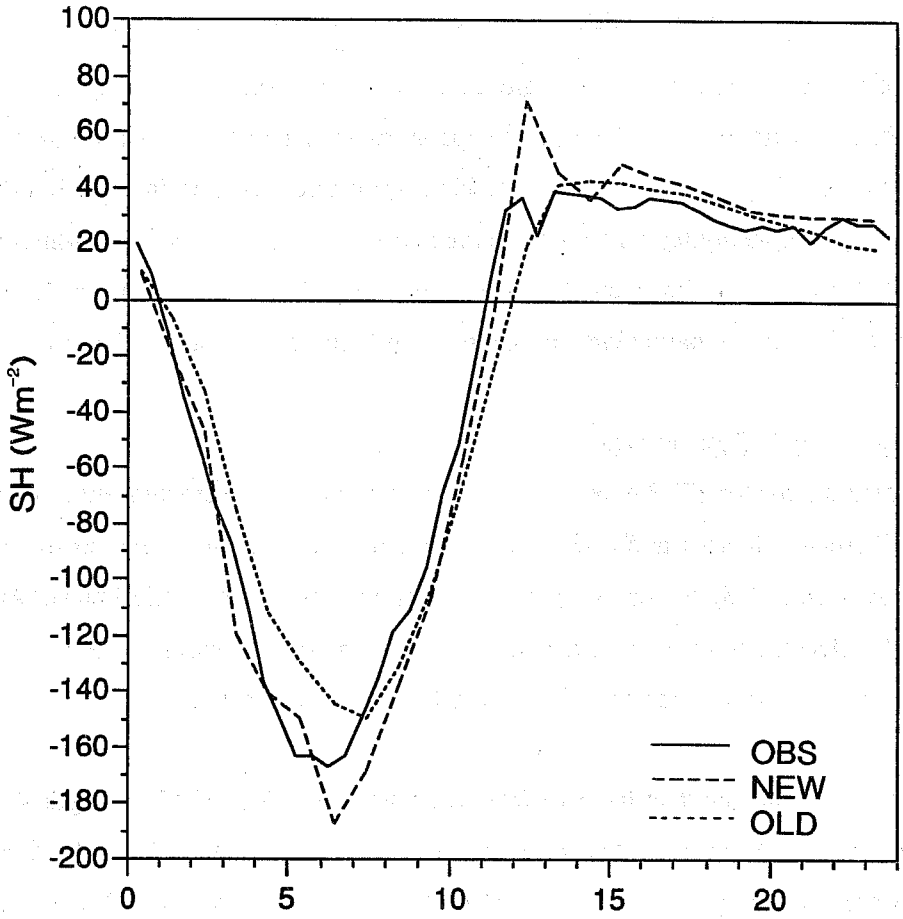

Fig. 20 As Fig. 18 for sensible heat flux.

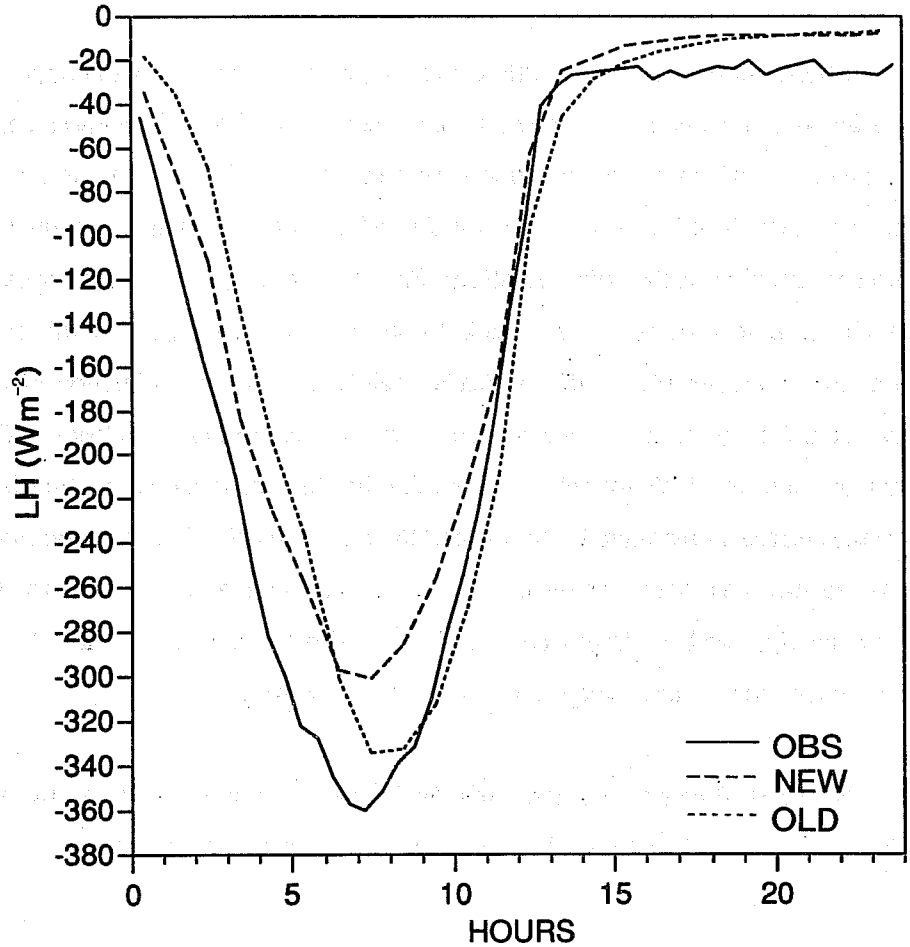

Fig. 21 As Fig. 18 for latent heat flux.

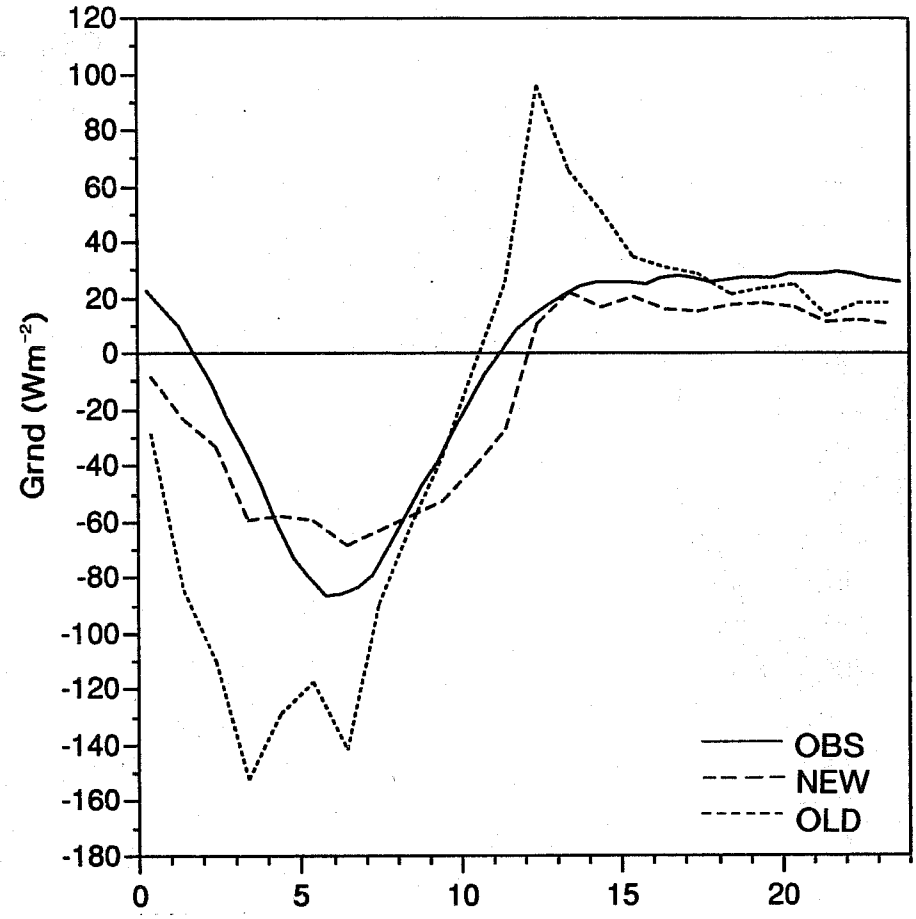

Fig. 22 As Fig. 18 for ground heat flux.

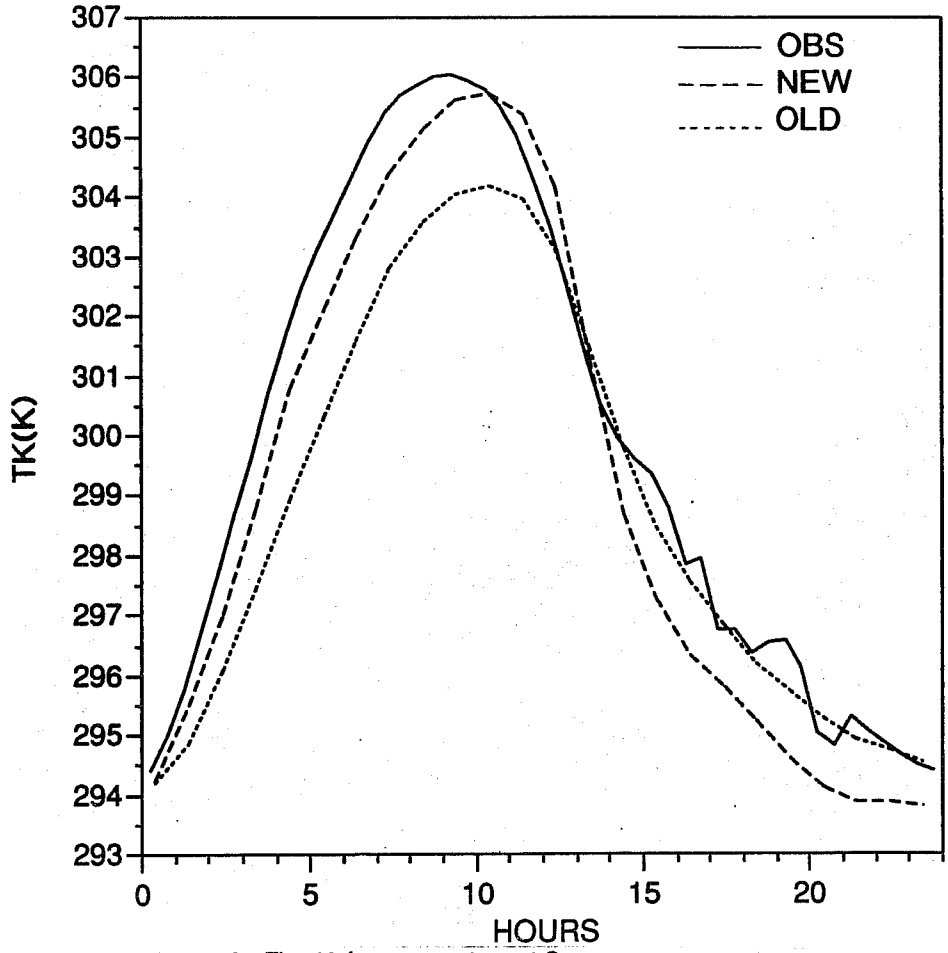

Fig. 23 As Fig. 18 for temperature at 2 m.

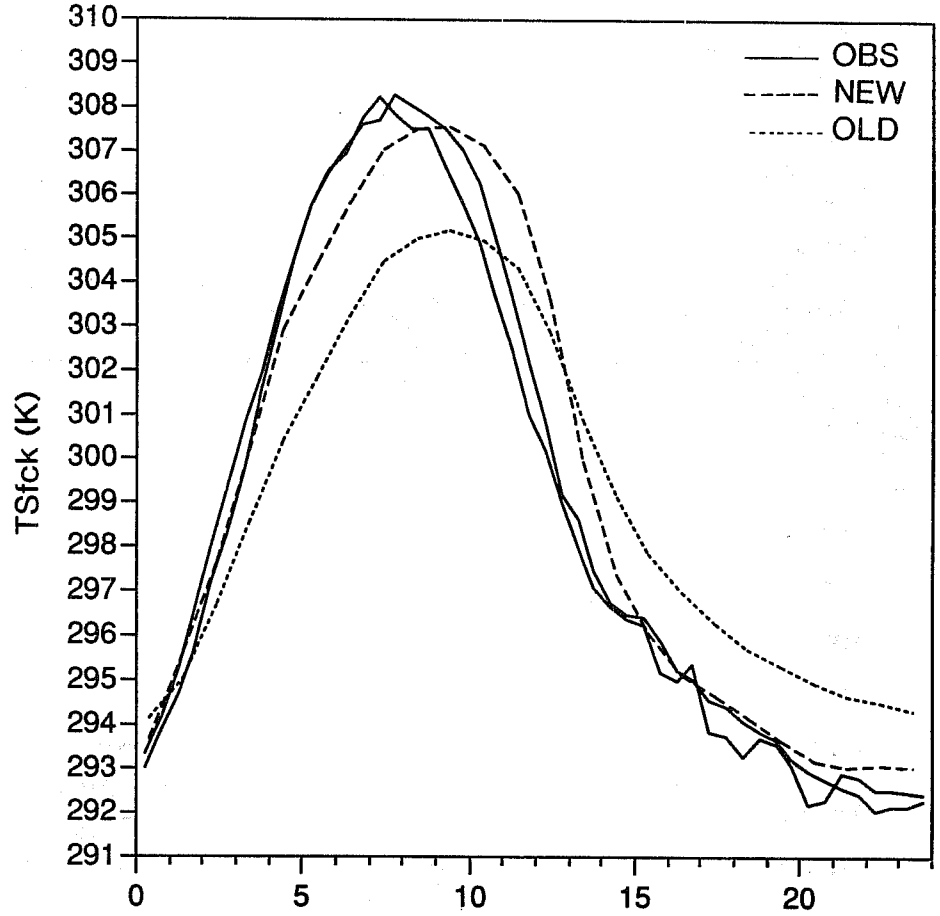

Fig. 24 As Fig. 18 for radiative surface temperature.

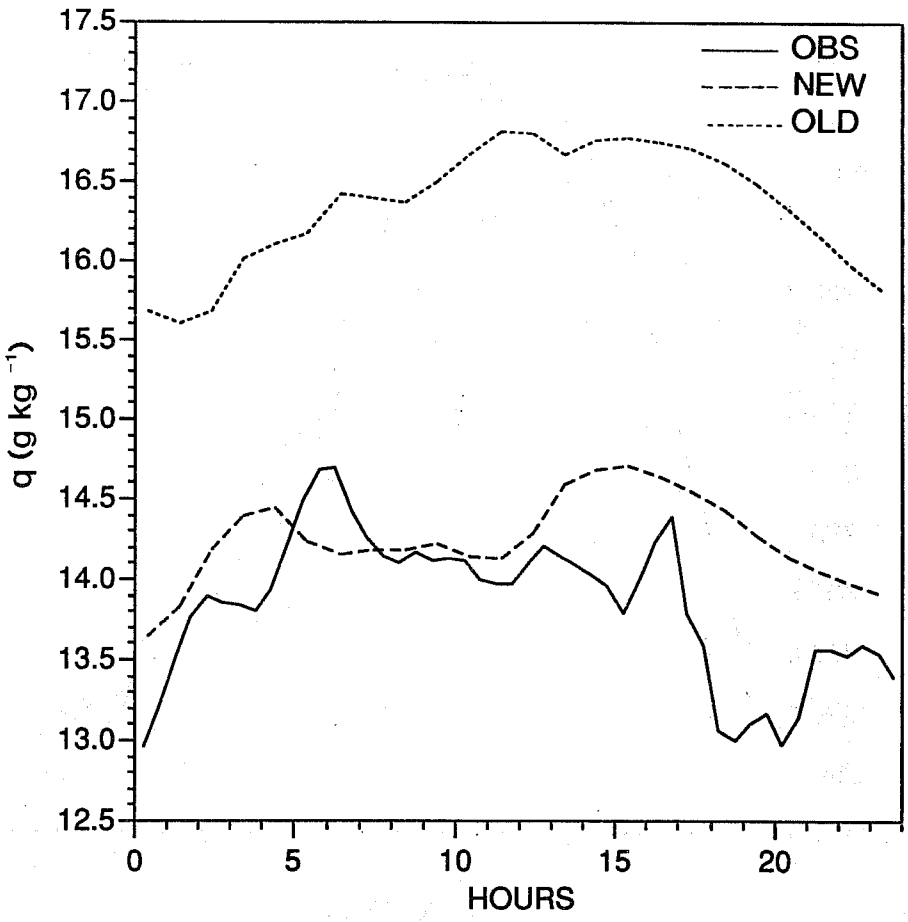

Fig. 25 As Fig. 19 for mixing ratio at 2 m.

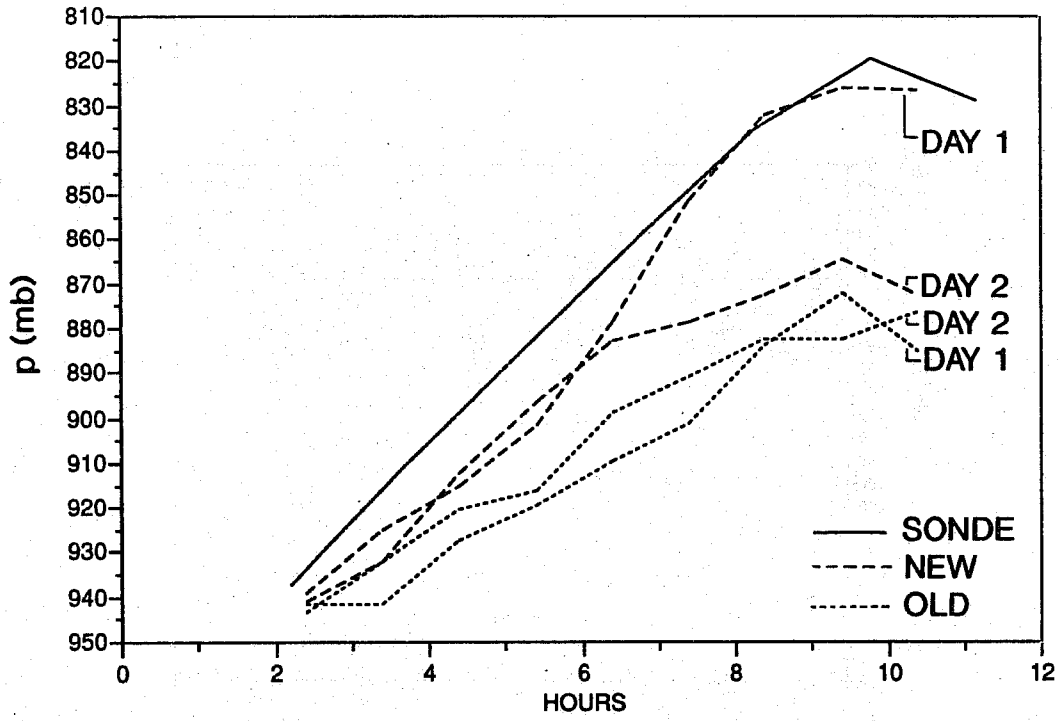

Fig. 26 Boundary layer top comparison from day 1 and 2 of the forecasts and from sonde data.

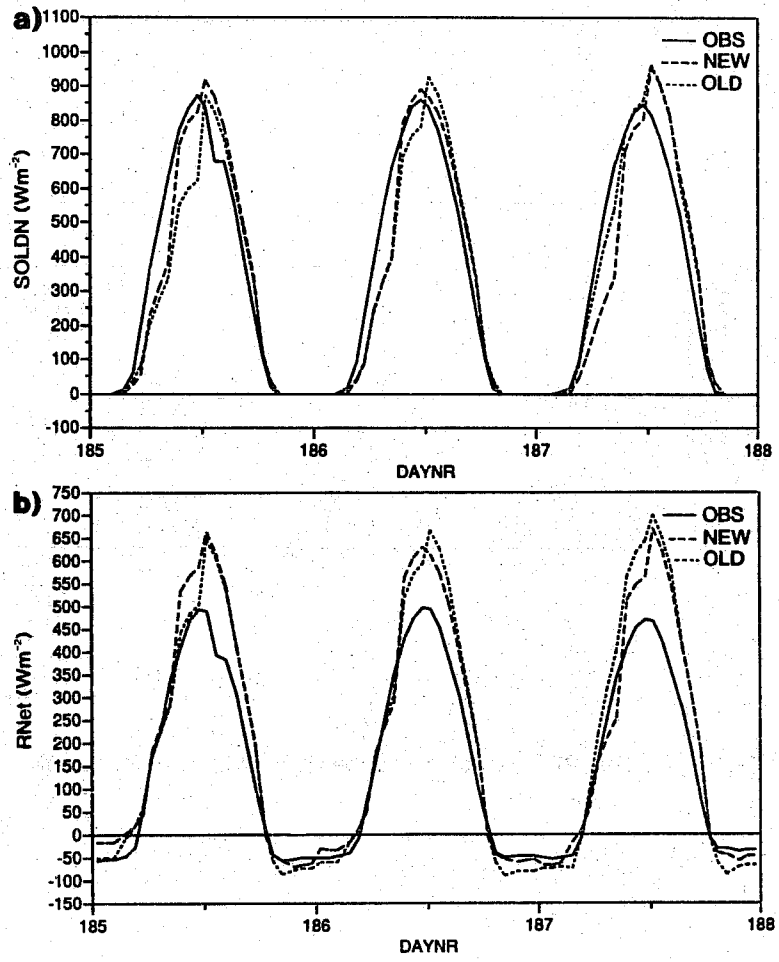

Fig. 27 Solar radiation (a) and net radiation (b) from 4 July 0000 GMT to 6 July 2400 GMT (Day 185, 186, 187) for Cabauw in The Netherlands in comparison with 12-36 hr forecasts started from 3-5 July 1200 GMT from the experimental re-analysis. The old as well as the new parametrization is used.

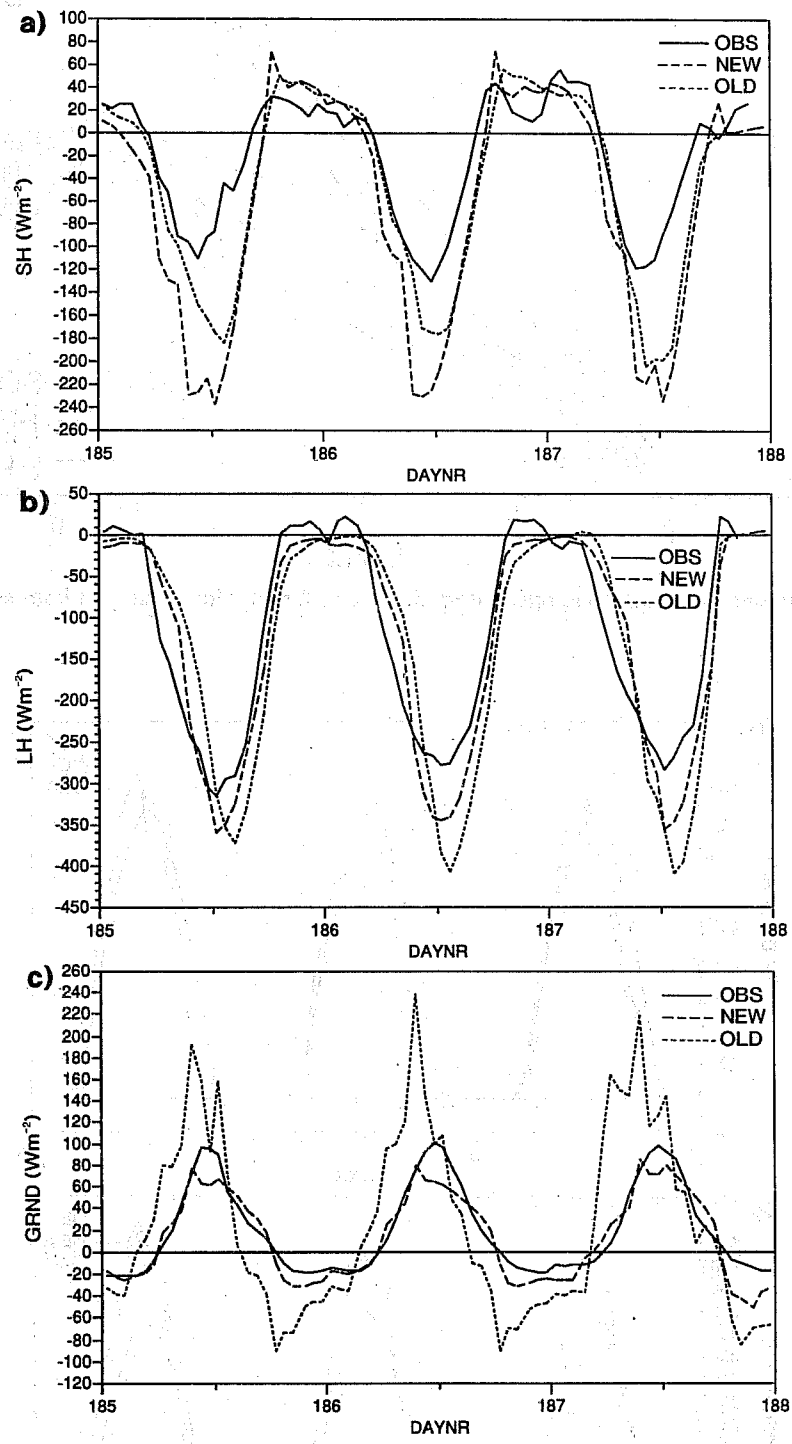

Fig. 28 As Fig. 27 for sensible (a) latent (b) and ground (c) heat flux.

worse. The ground heat flux from the old scheme shows similar problems as for the FIFE location. The new scheme gives results that are much closer to the data (Fig. 28c).

We will consider now diurnal cycles of the two lowest model levels in comparison with observations. Fig. 29a,b,c shows the horizontal wind speed together with the friction velocity (square root of surface stress divided by density). It is clear the new scheme follows the observed cycle much more closely than the old scheme. The model with the new scheme even reproduces the nighttime wind maximum which is the result of inertial oscillation after a reduction of frictional coupling with the surface. The old scheme produces too thick stable boundary layers and damps the inertial oscillation too much. The diurnal cycle in the friction velocity is more pronounced with the new scheme but still too weak, partly because the aerodynamic roughness length in the model is 2 to 3 times larger than representative for the Cabauw site.

The diurnal cycle of temperature at different levels is shown in Fig. 30. The amplitude of the diurnal cycle of the surface skin temperature is fairly close to the observations particularly with the new scheme. The phase error is due to the phase error in the radiative forcing caused by cloud problems. However, away from the surface, the data indicate a rapid decrease in amplitude, which is not captured by the model. At 150 m, the diurnal amplitude of the temperature is two times larger in the model than observed. A considerable part of this problem is due to the overestimation of the friction velocity from a too large surface roughness length.

Finally we show the mixing ratio at three heights in Fig. 31. The diurnal cycle in the mixing ratio is not very clear and fluctuations in the model forecast are hardly correlated with the data. The new scheme, however, produces a much better averaged mixing ratio than the old scheme, mainly as the result of the entrainment parametrization.

The comparison with Cabauw data shows similar model problems as the FIFE comparison. We mention: (i) the excessive forcing by the net radiation due to an overestimation of the clear sky solar radiation, an albedo bias and too little radiative response from the surface temperature, (ii) too large ground heat fluxes, and (iii) too moist boundary layers most likely due to the lack of entrainment. The problems with the surface temperature, the ground heat flux and the moisture were clearly alleviated with the new scheme. The possibility of comparing the diurnal cycle of the two lowest model levels with data lead to additional results: (i) The vertical structure of the diurnal cycle in wind is clearly improved with the new scheme; the reduction of momentum diffusion in the stable BL, allows an inertial oscillation that compares favourably with observations, and (ii) the diurnal cycle in the surface temperature is close to observations with the new scheme, but the coupling with the atmosphere is too strong; the diurnal amplitude in temperature at 150 m is too large compared with data.

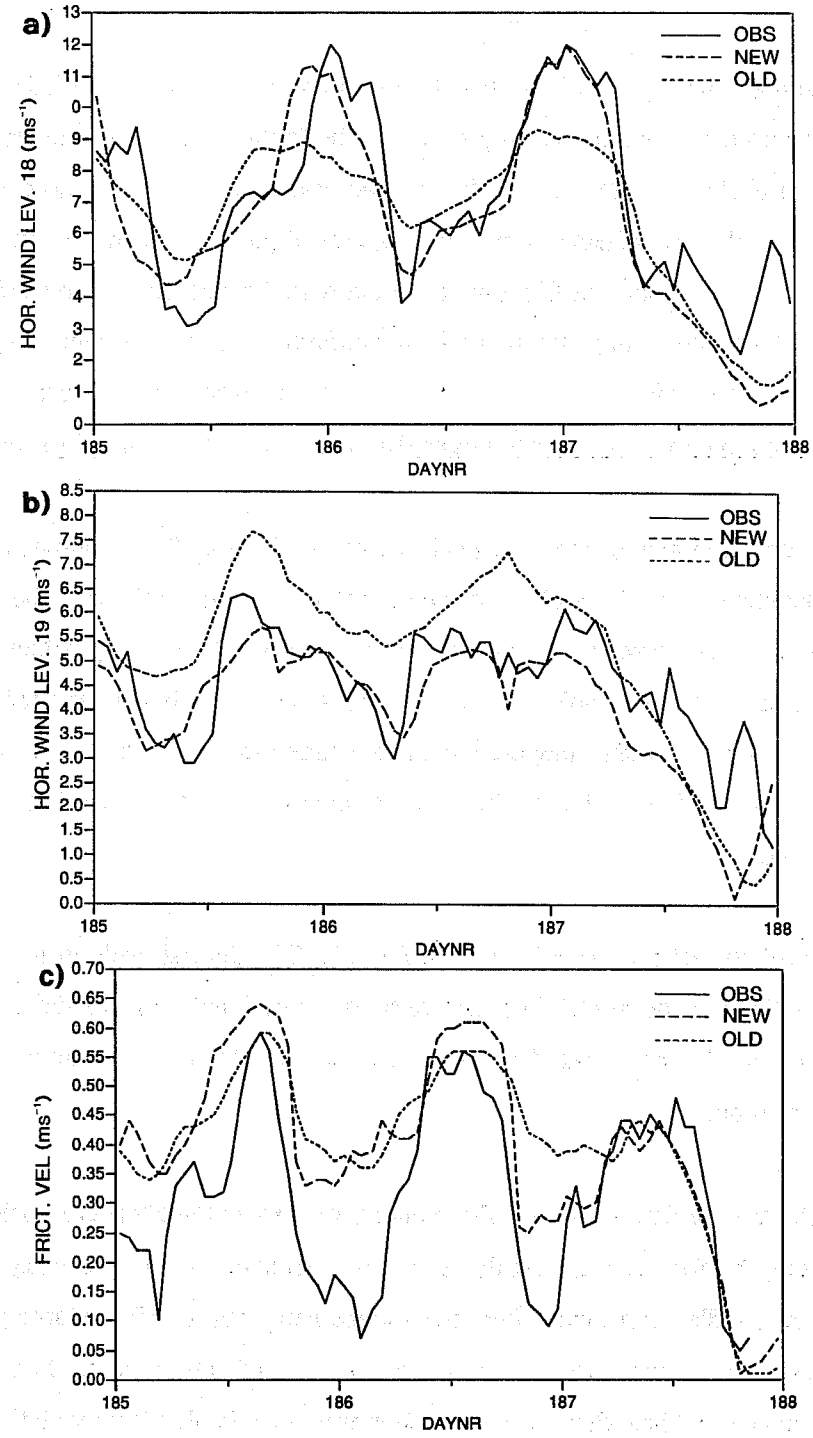

Fig. 29 As Fig. 27 for the horizontal wind speed of level 18 at about 150 m (a) and level 19 at about 30 m (b). Fig. c shows the friction velocity.

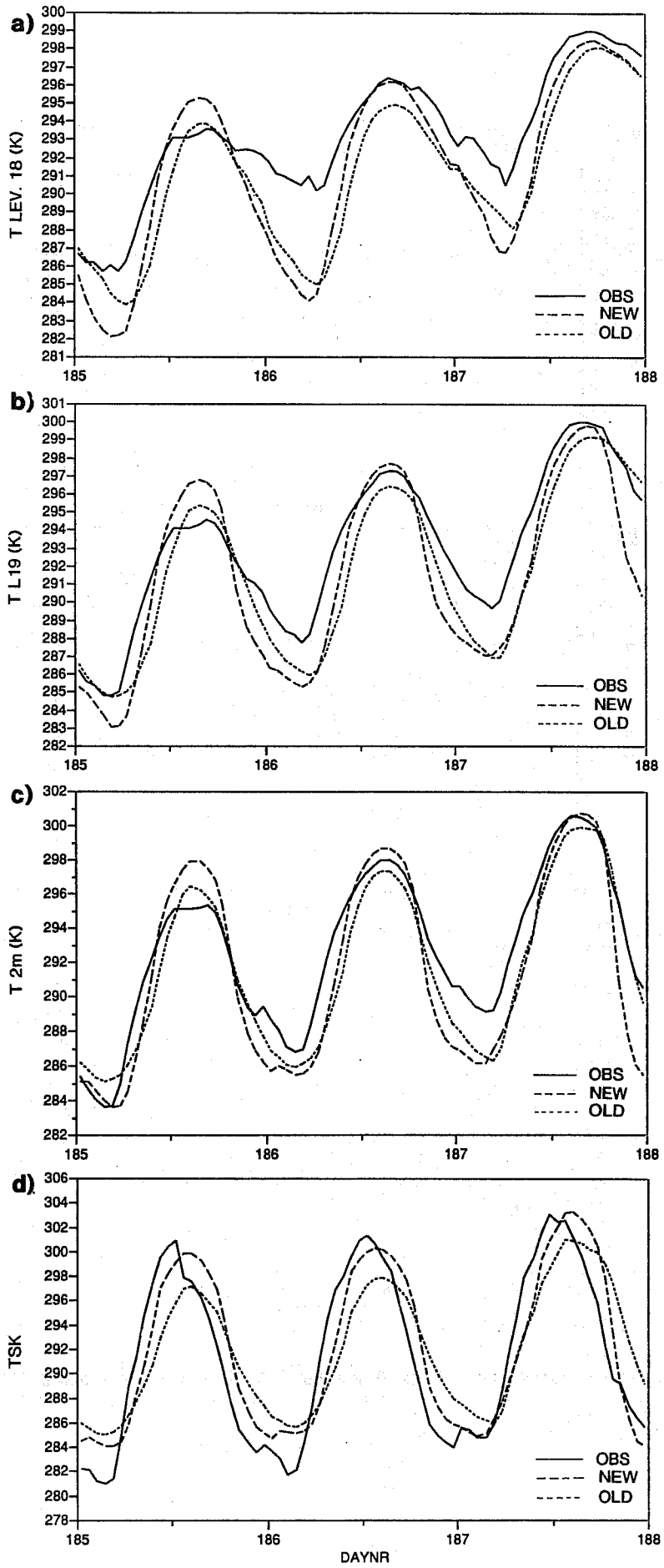

Fig. 30 As Fig. 27 for the temperature of level 18 at about 150 m (a), level 19 at about 30 m (b), 2 m (c) and at the surface (radiative surface temperature, d)

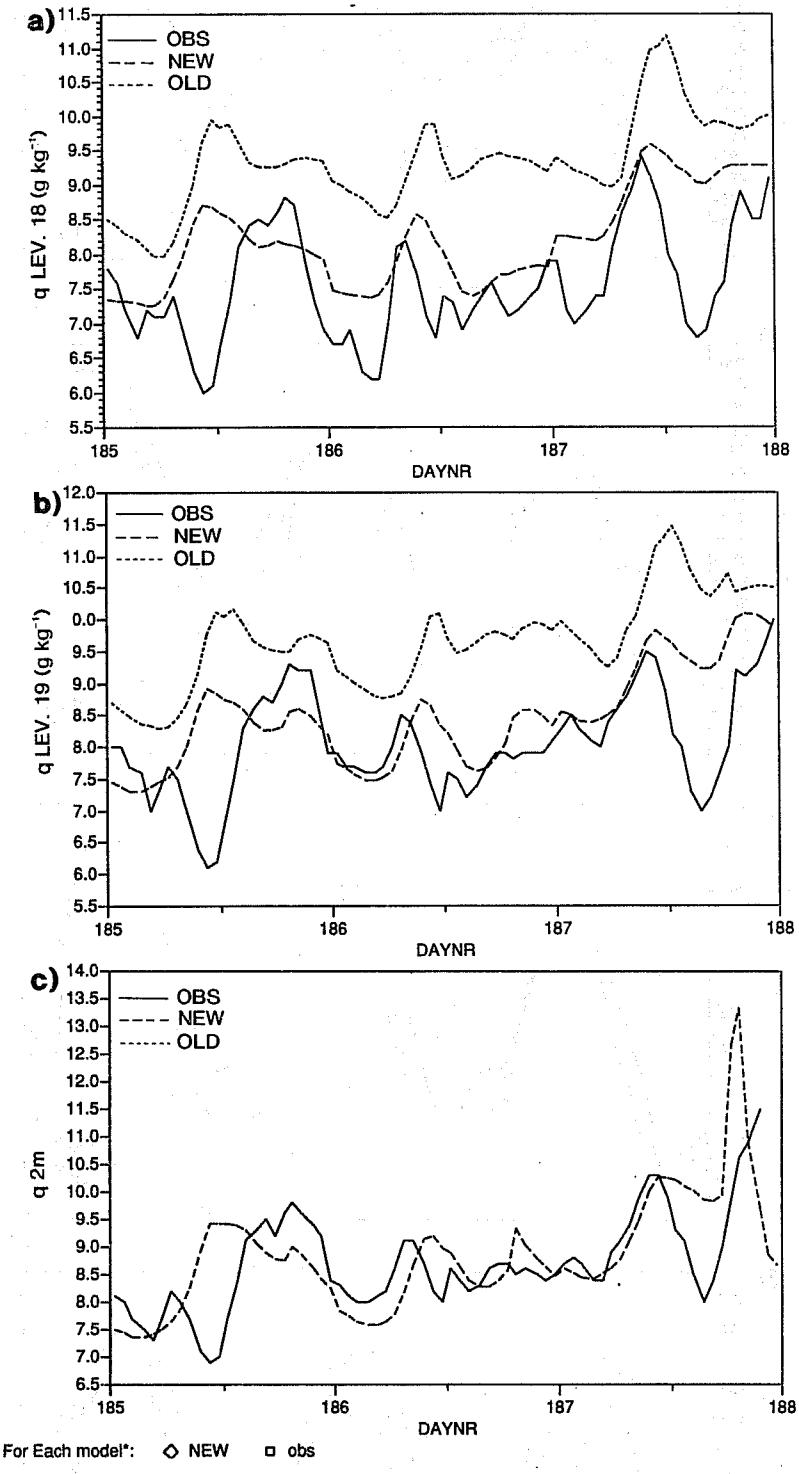

Fig. 31 As Fig. 27 for the mixing ratio of level 18 at about 150 m (a), level 19 at about 30 m (b), and 2 m (c).

4. Comparison of boundary layer parameters with radiosonde observations

For the period of October 1991 until August 1992, individual operational forecasts of boundary layer parameters have been compared with radiosonde observations. The resolution of the operational model for this period was T213L31. The distribution of model levels is roughly 30, 150, 350, 650, 950, 1350, 1800, 2250, 3300 ... metres above the model surface. The lowest 4 levels are at virtually the same height as in the 19-level model; above that the level spacing increases gradually to about 50 hPa in the 31-level model instead of 100 hPa in the 19-level model. The parameters we consider here are:

4.1 Inversion height

To determine the inversion height from sonde and forecast, the nearest gridpoint for a particular sonde is taken, the surface heat flux in the model is then recomputed from the model variables, and the inversion height is determined by the parcel lifting method described in section 3.3. This method is proposed by *Troen and Mahrt* (1986) as part of their parametrization scheme, but is used here for diagnostics (see also *Verver and Holtslag*, 1992). The same is done for the radiosonde data, but the model fluxes are used now as far as they are needed as scaling parameters in the inversion detection method. It has to be realized that the sensitivity to surface fluxes is relatively weak. Therefore crude estimates of the surface fluxes are quite sufficient for this application. The inversion heights that are shown are above local terrain for the sondes and above model orography for the model.

4.2 Temperature and mixing ratio

The temperature, mixing ratio and pressure of level 30 (about 150 m above the model surface) of the grid points, nearest to sonde stations, are taken and compared with the temperature and mixing ratio of the observation, interpolated to the model pressure. To simplify the interpretation, only those points are selected that have an upward heat flux in the model. The reason for selecting level 30 is that it is sufficiently far away from the surface to be in the well mixed layer and that it is sufficiently close to the surface to be below the inversion in most situations. We use this level to find "mixed layer" values.

Example scatter plots are shown in Fig. 32 for the sondes over Europe for the 48 hr operational forecast from 13 May 1992 12 GMT. The scatter in the results is large particularly for the inversion height. It should be realized however that the sonde profiles and the model profiles often have a structure that is much more complex than implied by a simple mixed layer concept. Errors in boundary layer cloud cover, can for instance lead to dramatically different BL structures and substantial errors in inversion height, BL temperature and BL mixing ratio. To summarize the BL biases and to get a feel of the evolution of these biases over the seasons, the errors in inversion height, BL temperature and BL mixing ratio are averaged over all the available sondes over Europe. This is done for the 2 day forecast of the 13th of every month, for the 4 day forecast of the 11th of every month and for the analysis of the 15th of every month. To

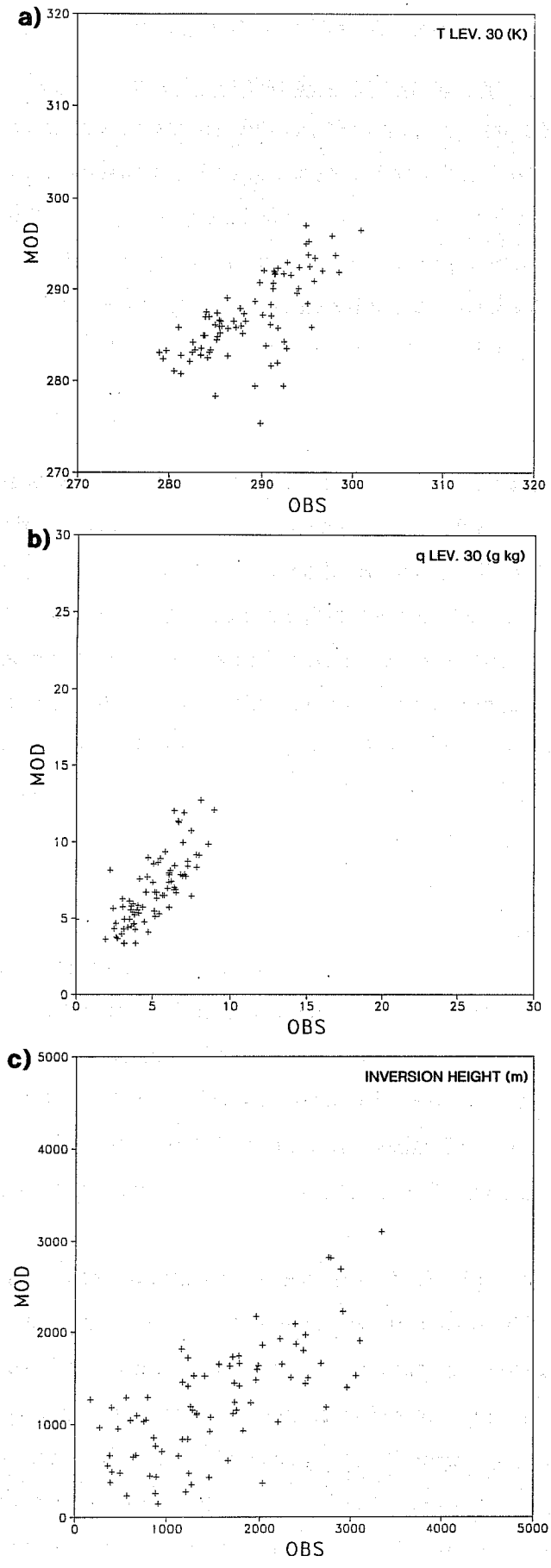

Fig. 32 Scatter plots (model against observations) of temperature at level 18 (a), specific humidity at level 18 (b) and inversion height (c) for all radiosonde locations between 35 N - 65 N and 10 W and 50 E. For the inversion heights, only locations with an an upward heat flux in the model are included. This example shows results of the operational 48 hour forecast from 13 May 1992 12 GMT in comparison with the 12 GMT sondes of 15 May.

increase the sample the 2 day forecast of the 3th of every month is also included. The mean bias over Europe for one forecast is shown as a single point in Fig. 33.

The evolution over the seasons of the model bias has a number of interesting aspects. First of all, we see little difference between the 2 day forecasts and 4 day forecasts and the analysis except for mixing ratio. For temperature and inversion height, the bias in the analysis is as large as in the forecasts. The reason is that, also in the analysis, the boundary layer structure is mainly determined by the model formulation and is not so much altered by the data. The analysis scheme will adjust the temperature over thick layers but will not correct for erroneous BL structures (e.g. sharp inversions). Secondly we see that the boundary layers are too moist most of the time except in August. Finally Fig. 33 suggests a correlation between BL temperature, mixing ratio and inversion height.

Although the systematic errors in the BL budgets are evident it is difficult to draw firm conclusions from Fig. 33. The budgets are affected by deficiencies in surface fluxes and entrainment, both of which can be in error. From the FIFE comparison we have seen a number of model problems that affect the BL budgets: (i) overestimation of net radiation at the surface in cloud free situations, (ii) lack of entrainment, and (iii) too much evaporation in wet soil conditions, rapid drying-out and too little or no evaporation in dry soil conditions. We can ask ourselves whether the seasonal evolution of BL biases can be explained in terms of the deficiencies mentioned above. We have to be cautious, because it is not to be excluded that biases in the cloud forecasts dominate the surface energy balance. The most remarkable tendency in the annual evolution of the BL biases is the transition from too shallow, too moist and too cold (or nearly bias free) BL's in April and May to too thick, too dry and too warm BL's in August. It is believed that the evolution of the soil water availability plays a crucial role here together with the entrainment. The lack of entrainment results in too shallow, too moist and too cold BL's in spring, but in summer the shortage of soil moisture dominates, resulting in deep, warm and relatively dry BL's. This interpretation implies that introduction of the entrainment parametrization without improving the soil hydrology will improve the model forecasts in spring, but will make the temperature and BL depth bias worse in summer.

5. CONCLUSIONS

We have compared the diurnal cycles of the ECMWF model with observations during FIFE and with Cabauw observations. A number of model deficiencies are evident from this comparison:

- The clear sky radiation is overestimated by about 8 %.
- The surface albedo is too low by a few percent for the FIFE location and perhaps by as much as 5 % for Cabauw.
- The ground surface model with a 7 cm thick layer responds too slowly to the radiative forcing.
- The diurnal amplitude of the radiative surface temperature is too small.

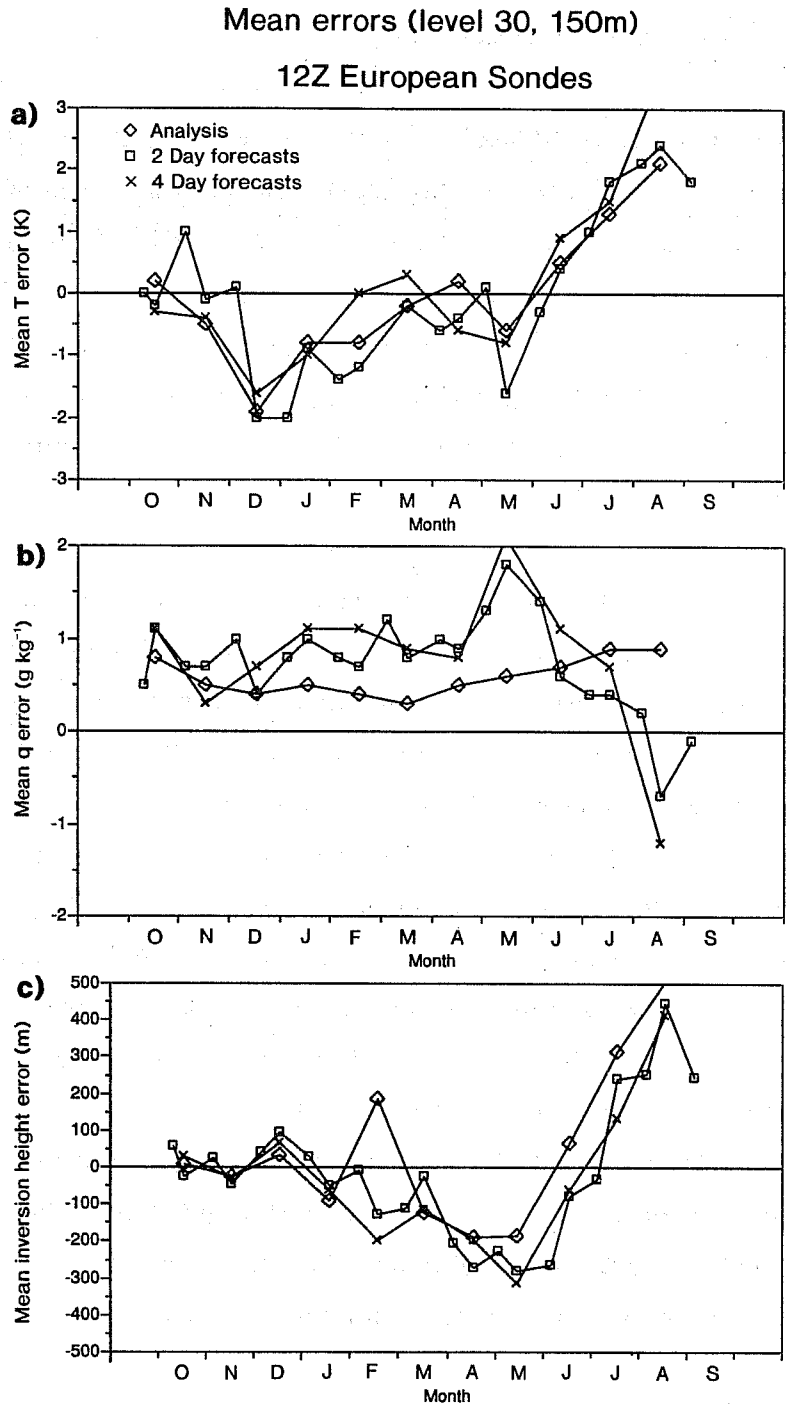

Fig. 33 Errrors of temperature (a) and specific humidity (b) at level 30 (about 150 m above the surface) and errors in inversion height (c) averaged over all sonde locations over the area between 35 N - 65 N and 10 W 50 E. The mean error for one forecast is represented by one point. For every month, two 48 hour forecasts, one 96 hour forecast and one analysis have been selected. For every month, the analysis, one of the 48 hr forecast and the 96 hour forecast have the same verifying date.

- The diurnal cycle of temperature at the lowest model levels is too strongly coupled to that of the surface.
- The model tends to dry out the soil too quickly after precipitation and evaporation tends to disappear completely at the end of the growing season.
- The BL lacks entrainment resulting in a tendency for the model to create shallow, cold and moist BL's.

The problem with the slow response of the surface to thermal forcing could easily be solved by introducing a parametrization for the skin temperature. Similarly a parametrization for boundary layer entrainment has been proposed, which is clearly beneficial to the BL structure, provided that the surface fluxes are correct.

The systematic bias in boundary layer structure found in the operational forecast has been interpreted in terms of model deficiencies. It appears that the introduction of the new BL scheme could be beneficial in spring when sufficient soil moisture availability does not hinder a reasonable estimation of the evaporation. In summer, however, so little soil moisture is available (probably due to erroneous climate values), that the lack of entrainment is compensated by excessive heat fluxes from the surface.

The present analysis clearly suggests systematic errors in the evaporative fraction at the surface. Examples are the lack of evaporation in October and the too short time scale for soil drying after precipitation. Another example is given by *Betts et al.* (1993), where it is shown that the August evaporation is too low when the operational soil moisture climate for August is used. The climate layer, acting as a fixed boundary condition in the layer between 49 and 91 cm deep, is believed to play a dominant role. The purpose of having a fixed deep soil climate is to prevent the model from drifting-away from realistic soil temperature and soil moistue. However, the comparison with FIFE data and the seasonal evolution of BL-errors suggest that the soil moisture climate is not very realistic. A further investigation of the soil hydrology scheme is currently in progress. Near surface time series of wind, temperature, mixing ratio, downward solar and thermal radiation and precipitation from FIFE, HAPEX and Cabauw will be used to drive the land surface scheme in a "stand alone single column" mode. This enables the study of the land surface scheme without interference from any other model problem. In the framework of these tests, it will be tried to replace the climatological layer by prognostic layer(s) with a zero flux condition in the deep soil.

References

Beljaars, A.C.M., 1988: Surface fluxes in moderately complex terrain, AMS, Proc. 8th Symp.Turb. Diff., 193-196, San Diego, Ca.

Beljaars, A.C.M., 1991: Numerical schemes for parameterizations. ECMWF Seminar proceedings, Sept. 1991, Numerical methods in Atmospheric Models, Vol. II, 1-42.

Beljaars, A.C.M. and A.A.M. Holtslag, 1991: On flux parametrization over land surfaces for atmospheric models, J.Appl.Meteor., 30, 327-341.

Betts, A.K., 1976: Modelling subcloud layer structure and interaction with a shallow cumulus layer. J.Atmos.Sci., 33, 2363-2382.

Betts, A.K., 1992: Budget analyses of the FIFE atmospheric boundary layer. J.Geophys.Res. (Atmos), 97, (in press).

Betts, A.K., R.L. Desjardins, J.I. MacPherson and R.D. Kelly, 1990: Boundary Layer Heat and Moisture Budgets from FIFE. Bound.-Layer Meteor., 50, 109-137.

Betts, A.K., R.L. Desjardins and J.I. MacPherson, 1992: Budget analysis of the Boundary Layer grid flights during FIFE-1987. J.Geophys.Res. (Atmos), 97, (in press).

Betts A.K. and J.H. Ball, 1992: FIFE-1987 mean surface data time series. Available on diskette from author (Atmospheric Research, Pittsford, VT 05763).

Betts, A.K. and A.C.M. Beljaars, 1992: Estimation of effective roughness length for heat and momentum from FIFE data. Submitted to Bound.-Layer Meteor.

Betts, A.K., J.H. Ball and A.C.M. Beljaars, 1993: Comparison between the land surface response of the European Centre Model and the FIFE-1987 data. Submitted to Quart.J.Roy.Meteor.Soc.

Blondin, C., 1991: Parameterization of land-surface processes in numerical weather prediction. Land surface evaporation, measurement and parameterization. Ed. T.J. Schmugge and J.C. André, Springer-Verlag, pp 31-54.

Driedonks, A.G.M., H. van Dop and W. Kohsiek, 1978: Meteorological observations on the 213 m mast at Cabauw in the Netherlands, Proc. 4th Symp.Meteor.Observ. and Instrum., April 1978, Denver, USA, AMS, Boston, p 41-46.

Garratt, J.R., 1978: Transfer characteristics for a heterogeneous surface of large aerodynamic roughness. Quart.J.Roy.Meteor.Soc., 104, 491-502.

Garratt, J.R. and B.B. Hicks, 1973: Momentum, heat and water vapor transfer to and from natural and artificial surfaces. Quart.J.Roy.Meteor.Soc., 99, 680-687.

Gash, J.H.C., J.S. Wallace, C.R. Lloyd, A.J. Dolman, M.V.K. Sivakumar and C. Renard, 1991: Measurements of evaporation from fallow Sahelian savannah at the start of the dry season. Q.J.R. Meteor.Soc., 117, 749-760.

Godfrey, J.S. and A.C.M. Beljaars, 1991: On the turbulent fluxes of buoyancy, heat and moisture at the air-sea interface at low wind speeds, submitted to AGU.

Holtslag, A.A.M., E.I.F. De Bruin and H.L. Pan, 1990: A high resolution air mass transformation model for short-range weather forecasting, Mon.Wea.Rev., 118, 1561-1575.

Kim, J. and S.B. Verma, 1990: Components of surface energy balance in a temperate grassland ecosystem. Bound.-Layer Meteor., 51, 401-417.

Louis, J.F., 1979: A parametric model of vertical eddy fluxes in the atmosphere. Bound.-Layer Meteor., 17, 187-202.

Louis, J.F., M. Tiedtke and J.F. Geleyn, 1982: A short history of the operational PBL-parameterization at ECMWF. Workshop on boundary layer parameterization, ECMWF, Nov. 1981, pp 59-79. (Available from ECMWF, Shinfield Park, Reading RG2 9AX, U.K.).

Miller, M., A.C.M. Beljaars and T.N. Palmer, 1992: The sensitivity of the ECMWF model to the parametrization of evaporation from the tropical oceans. To appear in J. Clim.

Mintz, Y. and Y.V. Serafini, 1989: Global monthly climatology of soil moisture and water balance. UNESCO Studies and Reports in Hydrology.

Sellers, P.J., F.G. Hall, D.E. Strebel and F.F. Murphy, 1988: The First ISLSCP field experiment (FIFE). Bull.Amer.Meteor.Soc., 69, 22-27.

Stewart, J.B. and S.B. Verma, 1992: Comparison of surface fluxes and conductances at two contrasting sites within FIFE area. J.Geophys.Res. (Atmos), 97, (in press).

Troen, I. and L. Mahrt, 1986: A simple model of the atmospheric boundary layer; sensitivity to surface evaporation, Bound.-Layer Meteor., 37, 129-148.

Verver, G.H.L. and A.A.M. Holtslag (1991): Sensitivity of an operational puff dispersion model to alternative estimates of mixed-layer depth, Proceedings of the 19th ITM on Air pollution modelling and its applications, Ierapetra, Greece.